Journal of Hydrology: Regional Studies 42 (2022) 101168

Contents lists available at ScienceDirect

Journal of Hydrology: Regional Studies

journal homepage: www.elsevier.com/locate/ejrh

Evaluating the performance of multiple satellite-based precipitation products in the Congo River Basin using the SWAT model

V. Dos Santos [a,*], R.A. Jucá Oliveira [b], P. Datok [a], S. Sauvage [a,*], A. Paris [b,c], M. Gosset [d], J.M. Sánchez-Pérez [a]

[a] Laboratoire Ecologie Fonctionelle et Environnement, Institut national polytechnique de Toulouse (INPT), Centre National de la Recherche Scientifique (CNRS), Université de Toulouse (UPS), Avenue de l'Agrobiopole, 31326 Castanet Tolosan Cedex, France
[b] Laboratoire d'Etudes en Géophysique et Océanographie Spatiales (LEGOS), UPS, CNRS, Centre National d'Etudes Spatiales (CNES), Institut de Recherche pour le Développement (IRD), 14 Avenue Édouard Belin, 31400 Toulouse, France
[c] Hydro Matters, 1 Chemin de la Pousaraque, 31460 Le Faget, France
[d] Geoscience Environnement Toulouse (GET), IRD, UPS, CNRS, CNES, 14 Avenue Édouard Belin, 31400 Toulouse, France

ARTICLE INFO

Keywords:
Precipitation
Satellite observations
FROGS
SWAT model
Congo River Basin

ABSTRACT

Study region: Congo River Basin
Study Focus: Precipitation is the major driving force of hydrological processes and is one of the main input datasets for hydrological models. The Congo River Basin is one of the least studied major river basins in the world and suffers from the scarcity and difficulty in accessing rain gauge data, necessitating the use of satellite precipitation estimates for hydrological studies. In this study, we have made a comprehensive comparison of different satellite-based precipitation products' inputs for a hydrological model in the Congo River Basin.
New hydrological insight for this region: Our findings showed that the products based on satellite-only source tend to overestimate the rainy season peaks in comparison with the 3B42_V7 product. On the other hand, the satellite products that consider gauge calibration presented better agreements between each other. The hydrological model was able to reproduce the general precipitation products characteristics, while the gauge-adjusted satellite products performed better than those without gauge adjustments. Overall precipitation patterns have a crucial effect on the model's performance and leads to different streamflow and water balance components' values. The choice of rainfall product has a significant importance in the interpretation of the simulated hydrological cycle.

1. Introduction

Hydrological models are frequently used as practical tools to assess and to predict the impacts of anthropogenic activities on water resources and also assist in their management or create a basis for decision-making on sustainable development alternatives and

* Corresponding authors.
E-mail addresses: van.c.dossantos@gmail.com (V. Dos Santos), rom.aug9@gmail.com (R.A.J. Oliveira), pankyesdatok@gmail.com (P. Datok), sabine.sauvage@univ-tlse3.fr (S. Sauvage), adrien.paris@hydro-matters.fr (A. Paris), marielle.gosset@ird.fr (M. Gosset), jose-miguel.sanchez-perez@univ-tlse3.fr (J.M. Sánchez-Pérez).

https://doi.org/10.1016/j.ejrh.2022.101168
Received 6 November 2021; Received in revised form 10 June 2022; Accepted 4 July 2022
Available online 18 July 2022

conservation practices (Abbaspour et al., 2015, Loucks and Beek, 2017). However, these models require distributed meteorological information (precipitation, temperature, wind speed, etc.), which is a great challenge in large and poorly gauged areas such as tropical regions.

Precipitation is one of the main parameters for hydrological models, but its estimation is still very difficult, because of its strong spatio-temporal heterogeneity (Beck et al., 2016). There are three ways of measuring precipitation over a basin: (i) conventional instrumentation, using networks of rain (or snow) meters; (ii) ground based weather radar; and (iii) satellite measurement. Nevertheless, despite the accuracy of estimates from conventional instrumentation and weather radar, the distribution and density of these methods are highly variable. Another issue with these methods is the completeness and consistency of the historical data series as well as the availability for near real-time analysis (Kidd and Levizzani, 2011; Sun et al., 2017). The precipitation data obtained by satellite is an alternative in regions where data is scarce, with a large number of free products available with high spatial and temporal resolution that can fill historical gaps and complement or replace in situ stations (Kidd et al., 2017). With the advent of the satellite Tropical Rainfall Measuring Mission (TRMM, Huffman et al., 2007), from late 1997–2014, transitioning with the launch of the Global Precipitation Measurement (GPM, Hou et al., 2014; Skofronick-Jackson et al., 2017) – a mission that is actually operating in conjunction with other passive microwave platforms- the performance of satellite precipitation estimates has significantly evolved along the years. Numerous satellite-based precipitation products, with different characteristics (i.e., spatial, temporal, among others), have since then been developed and improved for distinct application purposes, such as for climatological, hydrological, agricultural and monitoring studies. Numerous observational daily precipitation products, including satellite estimates, are now available in a common 1∘x1∘ grid format through the Frequent Rainfall Observations on GridS (FROGS) database (Roca et al., 2019). FROGS database enables easier intercomparisons and applications, based on the selection of a single to multiple products considering their category (i.e., satellite-only, gauge-adjusted satellite estimates, among others). Nonetheless, the estimation of satellite precipitation data is not wholly reliable due to the uncertainties arising from measurement errors associated with observations, sampling, recovery algorithms and bias correction processes that leads to systematic and random errors (Roca et al., 2010; Oliveira et al., 2016; Beck et al., 2016; Beck et al., 2017; Sun et al., 2017).

Tropical forests, including the Congo River Basin (CRB), strongly influence both the regional and global climate, storing large carbon stocks and regulating energy and water cycles. In this sense, any changes in the structure of these ecosystems, such as those caused by deforestation, can create positive feedbacks and increase climate change trends. The CRB in central Africa is the second-largest river basin in the world and supports one of Earth's three major humid tropical forest regions (Alsdorf et al., 2016); it contains about 70% of Africa's forest cover. Of the Congo Basin's 530 million hectares of land, 300 million are covered by forest. Almost 99% of the forested area is primary or naturally regenerated forest as opposed to plantations, and 46% is lowland dense forest. The average annual precipitation is around 1500–2000 mm of precipitation per year and is the most convectively active region of the world (Dezfuli, 2017). Almost 60% of precipitation occurs during the wet seasons and the basin-wide average seasonal cycle has two precipitation peaks, one in March and the other in November (Hua et al., 2019; Crowhurst et al., 2021). This basin is currently an object of concern because of evidence of a significant multidecadal drying trend, one of the most significant worldwide (Zhou et al., 2014; Harris et al., 2017). Despite the important role in the tropical climate system, the CRB is plagued by a scarcity of precipitation ground-data especially after the early 1990 s. This scarcity of data is primarily because the meteorological services of both Angola and the Democratic Republic of the Congo; countries that include most of the Congo rain forest, essentially ceased to function for decades and have been slow to rebuild their services (Alsdorf et al., 2016). The lack of in situ data leads most hydrological studies in the Congo basin to depend on satellite precipitation estimates.

Beighley et al. (2011), assessed the applicability of satellite precipitation estimates in terrestrial rainfall-runoff modelling in the CRB where three sources (products) of rainfall data were applied to the Hillslope River Routing (HRR) model. Although, large variability, among the products were found, especially in the equatorial regions of the CRB, the TRMM (3B42) product, which is a gauge-adjusted product, provided the best spatial and temporal distributions. However, the cause and potential solutions to the detected variability were not discussed by Beighley et al. (2011). On the other hand, Aloysius and Saiers (2017), in a climate projection context via rainfall-runoff model application, made use of 25 global climate models (GCMs) to explore the variability in modeled runoff in two subsequent periods (near future, 2016–2035 and mid-century, 2046–2065) and under two greenhouse gas emission scenarios. Aloysius and Saiers (2017), also revealed the importance of long-term and spatially explicit dataset for characterizing hydrologic response in minimizing the uncertainty that vary widely by region within the CRB, being crucial for both observational and projection studies.

This study aims to: (1) exploit the precipitation distributions and variability characteristics among the 23 gridded satellite-based precipitation products over the CRB, during the period from 2001 to 2012. The regional performance evaluations are categorized according to their input data sources (satellite-only and satellite gauge-adjusted), which leads to an unprecedented assessment over the region, that can provides important feedback to both the algorithm developers and science community on the support, for instance, of the climate, hydrological and agricultural monitoring and research. In addition, this study aims to analyze (2) the impact of these precipitation products inputs in a hydrological model, SWAT (Soil & Water Assessment Tool, Arnold et al., 1998) and investigate the potential behaviors of these different precipitation inputs in describing hydrologic processes. Although several hydrological models have been applied in the CRB (e.g.: Beighley et al., 2011, Tshimanga and Hughes, 2014), we considered the SWAT model because apart from its capability of simulating the water balance and storages in different compartments, it has demonstrated its flexibility for being appllied in several regions of the world (e.g.,: Tuo et al., 2016, Sharannya et al., 2020, Wang et al., 2021), in Africa (e.g.: Akoko et al., 2021) and in the Congo basin (Aloysius et al., 2017). This study will also contribute to the debate on the performance of satellite precipitation estimates in areas which lack in situ gauge measurements. Additionally, the utilization of a single product or an ensemble of products, in which the product characteristics are considered, as well as the precipitation product most appropriate in representing

the regional precipitation distributions, can be considered as subject of debate in multiple aspects (e.g., algorithm developments, research and monitoring applications).

The remainder of this paper is organized as follows: Section 2: we describe the study area, the precipitation database and the methodology. Section 3: provides an assessment and discussion of the selected precipitation products, which are subsequently applied through the SWAT model, and which are exploited in the same section. Finally, the conclusions are presented in Section 4.

2. Materials and Methods

2.1. Study Area and data

The intracratonic depression in Central Africa called the CRB (Fig. 1) is situated between latitudes 9°N and 14°S and longitudes 11°E and 34°E. It covers an area of approximately 3.7 million km^2 including most of the Democratic Republic of Congo, (DRC, formerly Zaire), the People's Republic of Congo (ROC) and the Central African Republic (CAR). Elevations within the basin are 3000 m above sea level (m asl) in the Eastern highlands and less than 300 m asl in the center of the basin (Runge, 2007). The physiography of the CRB

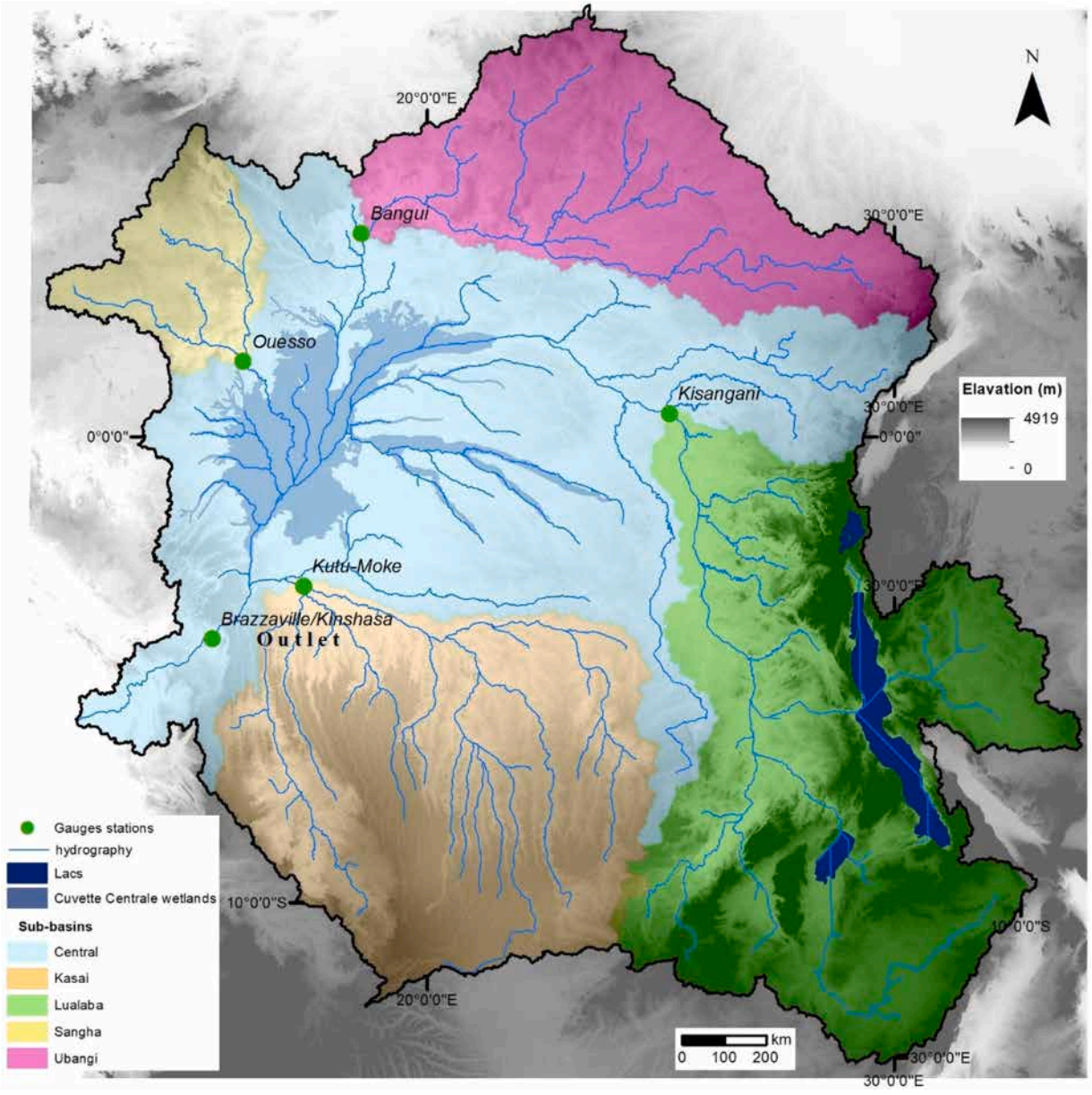

Fig. 1. Congo sub-basins studied. Also, the locations of gauge stations used in this study.

varies and consists of the northern peneplains of bushy/wooded savanna with tropical humid climate (Bultot, 1971). The middle basin includes the dense and heavily forested swamp forest of the Cuvette Centrale, and the sandy sandstone formations of the Batékés Plateaux of between 350 and 930 m altitude covered by bushy savanna (Laraque et al., 2001).

Mean annual rainfall is 2000 mm/y^{-1} in the central basin decreasing northward to southward to 1100 mm/y^{-1} (Alsdorf et al., 2016). The basic rainfall pattern across the basin is thought to be due to the bi-annual passage of the inter-tropical convergence zone (ITCZ) across the basin. The ITCZ over Africa is acknowledged as the location where the dry northeasterly harmattan meets the moist southerly flow of the monsoon and a major control on tropical rainfall. Recent evidence concerning the latitudinal progression of the equatorial rainy season however suggests that this view of the ITCZ may be challenged (Jackson et al., 2009; Nicholson et al., 2019). Rainfall across the basin occurs with a seasonal peak in Precipitation from December to March in areas of the southern hemisphere with northern hemisphere basins having theirs within July to October (Moukandi N'kaya et al., 2021). Annual extremes of precipitation in the equatorial regions are in April and October while sharp precipitation gradients, which may result in spurious trends, are noticed in the south-Eastern parts of the basin (Yin and Gruber, 2010; Tshimanga et al., 2012).

2.2. Satellite-based precipitation datasets

Twenty-three precipitation products, with a common period from 2001 to 2012 (except 3B42 v7.0, -period from 1998 to 2012), were selected for this study (Table 1). These datasets were acquired from The Frequent Rainfall Observations on GridS (FROGS) database (Roca et al., 2019). FROGS is composed of several quasi-global and regional daily precipitation products with a common spatial resolution of 1° × 1°. Although FROGS database includes satellites, ground-based and reanalysis products, only the satellite-based category was considered for this study. The satellite-based precipitation products, which differ from each other in multiple aspects (e.g., satellite source, with or without gauge adjustments, among others), are here sub-divided into two main groups: i) the satellite-only and ii) the gauge-calibrated satellite. These products are retrieved utilizing infrared (IR) observations from geo-stationary satellites and/or passive microwave observations from multiple or single low elevation orbiting (LEO) satellites. The gauge-based calibration step is distinctly applied to those satellite precipitation products. These adjustments are climatological on a monthly or daily time step and take into consideration in-situ observations from the Global Telecommunication System (GTS) or other gauged-based precipitation products (e.g., GPCC). Table 1 shows the satellite-based precipitation products selected for this study and their main characteristics. FROGS database is freely available from ftp://ftp.climserv.ipsl.polytechnique.fr/FROGs/. See Roca et al. (2019) for a detailed description of each product.

2.3. SWAT Model

The soil & Water Assessment Tool is a continuous-time, spatially distributed hydrological basin scale model that simulates water,

Table 1
Summary of the selected satellite-based precipitation products used in the present study. * Multiple platforms and # Single platform.

Type of data	Satellite source	#	Product short name and version	Temporal coverage	Spatial coverage	Reference
Satellite-only (10)	IR+MW*	1	IMERG v6.0 - Early	2000–2018	60° N-S	Huffman et al. (2019)
	IR+MW*	2	IMERG v6.0 - Late	2000–2018	60° N-S	Huffman et al. (2019)
	IR+MW*	3	IMERG V06 - Final Uncal	2000–2018	60° N-S	Huffman et al. (2019)
	IR+MW*	4	3B42 RT v7.0 uncalibrated	2000–2017	50° N-S	Huffman et al. (2007)
	IR+MW*	5	GSMaP-RNL - no gauge v6.0	2001–2013	50° N-S	Kubota et al. (2007)
	IR+MW*	6	GSMaP-NRT - no gauge v6.0	2001–2017	50° N-S	Kubota et al. (2007)
	IR+MW*	7	CMORPH v1.0 RAW	1998–2017	60° N-S	Xie et al. (2017)
	MW*	8	3B42 v 7.0 MW	1998–2018	50° N-S	Huffman et al. (2007)
	IR	9	3B42 v7.0 IR	1998–2018	50° N-S	Huffman et al. (2007)
	IR	10	CHIRP v2.0	1981–2016	50° N-S	Funk et al. (2015)
Gauge-calibrated satellite (13)	IR+MW*	11	IMERG v6.0 - Final Cal	2000–2018	60° N-S	Huffman et al. (2019)
	IR+MW*	12	3B42 v7.0	1998–2018	50° N-S	Huffman et al. (2007)
	IR+MW*	13	3B42 RT v7.0	2000–2017	50° N-S	Huffman et al. (2007)
	IR+MW*	14	GSMaP-RNL - gauge v6.0	2001 – 2013	50° N-S	Kubota et al. (2007)
	IR+MW*	15	GSMaP-NRT - gauge v6.0	2001–2017	50° N-S	Kubota et al. (2007)
	IR+MW*	16	CMORPH V1.0 CRT	1998–2017	60° N-S	Xie et al. (2017)
	IR+MW#	17	GPCP 1DD CDR v1.3 (yes_enforced)	1997–2017	90° N-S	Huffman et al. (2001)
	IR+MW#	18	GPCP 1DD CDR v1.3 (not_enforced)	1997–2017	90° N-S	Huffman et al. (2001)
	IR	19	PERSIANN CDR v1 r1	1983–2017	50° N-S	Ashouri et al. (2015)
	IR	20	CHIRPS v2.0	1981–2016	50° N-S	Funk et al. (2015)
	IR	21	TAMSAT v2.0	1983–2017	Africa (Land only)	Maidment et al. (2017)
	IR	22	TAMSAT v3.0	1983–2017	Africa (Land only)	Maidment et al. (2017)
	IR	23	ARC v2	1983–2017	Africa (Land only)	Novella and Thiaw (2013)

sediment, nutrient, chemical, and bacterial transport in a basin resulting from the interactions among weather condition, soil properties, stream channel characteristics, vegetation and crop growth, as well as land-management practices. The model calculates pollutant loads from various non-point and point sources (Arnold et al., 1998). Fundamentally, the model is hydrologically driven, based upon the water balance of an individual landscape unit:

$$SW_t = SW_0 + \sum_{i=1}^{t} \left(R_{dayi} - Q_{surfi} - E_{ai} - w_{seepi} - Q_{gwi}\right) \quad (1)$$

where SW_t is the final soil water content (mm H_2O); SW_0 is the initial soil water content (mm H_2O); t is time (days); R_{dayi} is precipitation on day i (mm H_2O); Q_{surfi} is surface runoff on day i (mm H_2O); E_{ai} is evapotranspiration on day i (mm H_2O); w_{seepi} is the amount of water from the soil profile inflowing to the vadose zone on day i (mm H_2O); and Q_{gwi} is the base flow on day i (mm H_2O).

2.3.1. Model Setup

SWAT2012 version (Winchell et al., 2013) was setup for the CRB using the datasets listed in Table 2. The basin was delineated based on the dominant land use, soil and slope classes taking into cognizance the size and spatial heterogeneity of the basin allocating one Hydrologic Response Unit (HRU) per subbasin resulting in 272 subbasins and HRUs. The period of simulation was from 1998 to 2012, comprising calibration (2000–2006), validation (2006–2012), and a two-year warm-up period (1998–2000). Lakes, wetlands and reservoirs were setup in SWAT model. The reservoirs were parameterized based on available information and assuming that no management system was in place.

In the SWAT model, the evapotranspiration is calculated using the Penman-Monteith method. The Penman-Monteith method also gave better estimates of evapotranspiration when used with the plant growth modification of Strauch and Volk (2013). The plant growth module was used since the SWAT model simulates plant growth based on dormancy during the winter season for the reinitiation of the growing season for perennial plants and this process is not a valid growing pattern in the tropics. The surface runoff was calculated using the Soil Conservation Service's Curve Number method (USDA Soil Conservation Service, 1972) and the variable storage method (Williams, 1969) was used for channel routing.

2.3.1.1. Wetland. The choice of model is explained in Datok et al. (2022), but in order to further emphasise the assumptions made in this study, it is important to underline that the level of complexity and types/quality of data needed for the model (Datok et al., 2022) informed the choice of the model. The main assumption made was to treat the central wetland area as a blackbox, thus creating a deterministic model that may not take into account all physical processes. The SWAT model is a process based model simulating both upland and channel processes. The land phase is solved at HRU level in which the hydrologic cycle controls the amount of water, sediment, nutrient and pesticide loadings to the main channel and (ii) a stream phase solved at reach level where water, sediments and nutrients move through the channels of the watershed to the outlet. Being semi-distributed, the internal variables of the model are adjusted based on a combination of unit cells whose location is not precisely located. Since small-scale spatial differences were not needed, we relied on basin-scale or regional parameters to calibrate the model.

Wetlands and depressions are located in subbasins off the main channel, thus water that flows into them must originate from the subbasin they are located. For reservoirs, they are located on the main channels, thereby trapping all flow from upstream subbasins (Neitsch et al., 2011). In our model, the watershed was partitioned into 272 subbasins where an unequal number of subbasins drained to each of the four principal gauging stations while the entire watershed drained into the main gauging outlet at Brazzaville Kinshasa. Since the 272 subbasins had an equal number of HRUs for reasons given in Datok et al. (2022), it meant that the hydrological effects of the wetlands are proportionally distributed within the respective HRUs. Thus, the model offers future promise as the availability of observations in any one of the wetland subbasins will seriously improve the model calibration. The water balance for the wetland in SWAT is given as follows:

$$V = V_{stored} + V_{flowin} - V_{flowout} + V_{pcp} - V_{evap} - V_{seep} \quad (2)$$

Table 2
Description of the nature and source of datasets employed in the SWAT Model.

Data Type	Period	Resolution	Source
Digital Elevation Model (DEM)	2008	90 m	Consortium for spatial information (https://cgiarcsi.community/data/srtm-90 m-digital-elevation-database)
Soil	2012	1 km	Harmonized World Soil Database v 1.1 (http://webarchive.iiasa.ac.at/Research/LUC/External-World-soil-database/HTML/index.html?sb=1)
Land use	2000	1 km	Global Land Cover 2000 database (http://forobs.jrc.ec.europa.eu/products/glc2000/products.php)
Meteorological data [daily temperature (min., max.), solar radiation, relative air humidity, wind speed]	1998 – 2012	~38 km	Climate Forecast System Reanalysis (CFSR) Model (http://rda.ucar.edu/pub/cfsr.html & http://globalweather.tamu.edu/) Dile and Srinivasan (2014)
Precipitation data [TMPA(TRMM) 3B42 v7.0]	1998–2015	0.25°	Huffman et al. (2007)
River discharge	2000 – 2012	Daily	SO-HYBAM (http://www.so-hybam.org/);BRLi (2016)

where V is the volume of water in impoundment at the end of the day (m^3 H_2O); V_{stored} is the volume of water at the beginning of the day (m^3 H_2O); V_{flowin} is the volume of water entering the wetland during the day (m^3 H_2O); $V_{flowout}$ is the volume of water flowing out of the wetland during the day (m^3 H_2O); V_{pcp} is the volume of precipitation falling on the wetland during the day (m^3 H_2O); V_{evap} is the volume of water removed from the wetland during the day (m^3 H_2O); and V_{seep} is the volume of water lost from the wetland during the day (m^3 H_2O).

In calculating the inflows into the wetlands, SWAT subtracts the volume of water entering the wetland from the surface runoff, lateral flow and groundwater loadings to the main channel. On the other hand, the wetland releases water whenever the water volume exceeds the normal storage volume:

$$V_{flowout} = 0 if V < V_{nor} \quad (3)$$

where V_{nor} is the volume of water held in wetland when filled to the normal water level (m^3 H_2O) (Neitsch et al., 2011).

2.3.1.2. 3B42 v.7 reference database. SWAT model was setup with daily precipitation estimates by the TMPA 3B42 v.7 product from the Tropical Rainfall Measuring Mission (TRMM) (afterward 3B42). The 3B42 v.7 provides rainfall estimates at a 3-h temporal resolution and 0.25° × 0.25° spatial resolution daily grids that spans nearly three decades (1998 – today). The quality of the TMPA 3B42 product has been assessed for several tropical regions, some of them focusing on the CRB (Munzimi et al., 2015 and 2019; Washington et al., 2013). Studies such as Munzini et al. (2015), demonstrate that despite some of the limitations in validating satellite-based products, the 3B42 v.7 is consistent in the depiction of intra-annual variation in CRB.

We chose the 3B42 v.7 instead of the gauge stations to set-up the SWAT model firstly, because there is a low gauge density across the CRB (Munzimi et al., 2015, Kabuya et al., 2020), and secondly, the gaps or missing data after the 80's (Samba et al., 2008 and Nicholson et al., 2019.) Spatial and temporal rainfall data scarcity has a large impact on general and extreme streamflow simulations (Tan and Yang, 2020). As well, this scarcity would lead to errors in trend analysis. In this context, 3B42 v.7 was more suitable to be used as input for SWAT model.

2.3.2. Model calibration

Model calibration was based on the optimization of the parameter values by adjusting the simulated streamflow (Q_{sim}) to observed streamflow (Q_{obs}) at a monthly time step. The observed data from the five gauging stations (Fig. 1) are located on major tributaries of the CRB, two on the northern side of the basin (Ubangui at Bangui and Sangha at Ouesso), two others on the southern side (Lualaba at Kisangani and Kutu-Moke at Kasai), and the fifth station is located at the Brazzaville/Kinshasa gauging station that controls 98% of the entire basin. The common period of calibration and validation for the stations was taken as the years 2000–2012 (Table 2).

In the model set-up used, the simulated streamflow was adjusted to the observed streamflow by manual calibration (trial and error). This method follows the simple approach of manual adjustment of uncertain or unknown parameters and the comparison of predictions with measured values relying on human judgment to attain the best fit for model parameters (Moradkhani and Sorooshian, 2008). The model parameterization was done by adjusting influential parameters: firstly, parameters, which are generally sensitive, such as groundwater-related parameters; secondly, parameters related to runoff, infiltration and evapotranspiration (Table 3). The parameters were regionalized according to the characteristics of the subbasins. Further details of the calibration and validation procedures can be found in Datok et al. (2022).

For the evaluation of model performance, we used the Nash and Sutcliffe (1970) efficiency (NSE) that measures the magnitude of residual variance, compared to observed variance (Moriasi et al., 2007); the coefficient of determination (R^2) that describes the degree of linear relationship between observed and simulated streamflow and percent bias (PBIAS) which evaluates the average tendency of the magnitude of simulated values in relation to the observed ones. The Kling–Gupta efficiency (KGE) by Gupta et al. (2009), is a decomposition of the NSE and mean squared error. KGE facilitates the analysis of relative importance of correlation, bias, and variability in hydrologic modeling (KGE-hydroGOF, 2017). For streamflow, Moriasi et al. (2015) proposed NSE values > 0.50, $R^2 > 0.60$

Table 3
SWAT parameters used for calibration (adapted from Datok et al., 2022).

Parameter (model file)	Parameter description	Process	Default value	Calibrated range
CANMX (.hru)	Maximum canopy storage (mm H_2O)	Interception	0	50–250
ALPHA_BF (.gw)	Base flow alpha factor (days).	Groundwater	0.048	0.002–0.016
GW_DELAY (.gw)	Groundwater delay: time required for water leaving the bottom of the root zone to reach the shallow aquifer (days)	Groundwater	31	31
GWQMN (.gw)	Threshold depth of water in the shallow aquifer required for return flow to occur (mm H_2O)	Groundwater	1000	500–1000
GW_REVAP (.gw)	Groundwater "revap'' coefficient: controls the amount of water which evaporates from the shallow aquifer (-)	Groundwater / evapotranpiration	0.02	0.02–0.12
REVAPMN (.gw)	Threshold depth of water in the shallow aquifer for "revap'' to occur (mm H_2O)	Groundwater / evapotranpiration	750	0.002
RCHG_DP (.gw)	Deep aquifer percolation fraction (-)	Groundwater	0.05	0
CH_N2 (.rte)	Manning's "n" value for the main channel	Routing	0.014	0.014–0.06
CH_N1(.sub)	Manning's "n" value for tributary channels	Routing	0.014	0.014–0.06

and PBIAS $< \pm 25$ to be a satisfactory level for monthly scales. A KGE value > 0.50 is also considered satisfactory (Gupta et al., 2009).

2.4. Evaluation of the performance of precipitation datasets using SWAT model

The SWAT model was run for twenty-three scenarios based on the precipitation products described in Table 1. The base scenario is based on the 3B42_v7.0 product and it was calibrated with observed streamflow (see above). The other precipitation scenarios were run using identical datasets (see Table 1) so that variations in streamflow and other hydrological components were uniquely attributable to precipitation. For the evaluation of the performance of precipitation datasets, we used KGE and PBIAS objective functions calculated using the streamflow of base scenario (3B42_v7.0) as reference.

3. Results and discussion

Precipitation regimes over the CRB are firstly assessed through the 23 satellite-based precipitation products during the period from 2001 to 2012. Secondly, the model calibration and validation are performed for the period from 1998 to 2012 (two-years of warm-up for the model). Afterwards, hydrological evolution (streamflow and water balance components) through the 23 precipitation products during 2003–2012 (two-years of warn-up) are assessed. Finally, we discuss the influence of the precipitation input on model performance when the model has been pre-calibrated with one of the products (here 3B42).

3.1. Comparison of the different precipitation datasets

Satellite precipitation estimates, through different gridded products, has been constantly evaluated and assessed across West Africa, considering gauged-precipitation observations as a reference (e.g., Gosset et al., 2018, Nicholson et al., 2019, Satgé et al., 2020). The reliability of satellite precipitation estimates depends on several factors (e.g., seasonality, the gauge network densities) and can vary in space and time. The precipitation regime (i.e., seasonality) over the CRB varies regionally (e.g., Munzimi et al., 2015). Spatially, there are remarkable characteristics on the precipitation distribution over CRB, which are demonstrated through the unconditional annual mean and the 99th percentile (Fig. 2). The central region of the CRB and the northern portion of the Luabala sub-basin experience the largest amounts of precipitation with about 7 and 10 mm day-1, respectively. Nevertheless, the Lualaba also showed the largest regional contrast of precipitation amounts, with most of the watershed area presenting precipitation mean lower than 3 mm day^{-1}. These spatial characteristics were directly linked to the extreme precipitation occurrences, represented by the 99th percentile, strongly influenced by the surface type (i.e., orographic) conditions, where the highest values (>50 mm day^{-1}) were found mainly across the wetland zones and over the northwest part of Lualaba. Fig. 3 depicts the annual cycle of precipitation, through the monthly accumulated mean distributions, from all the selected satellite-based precipitation products over the five CRB sub-basins, during the period from 2001 to 2012. The contrasts between the satellite-only and satellite gauged-adjusted precipitation are

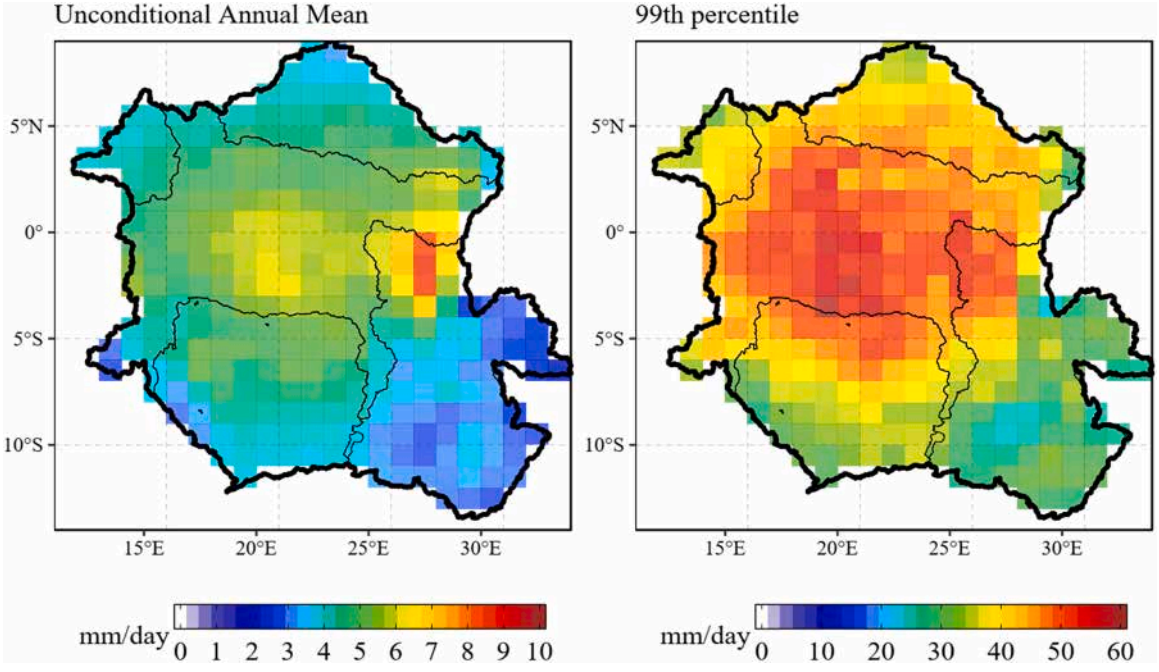

Fig. 2. The spatial distribution of a) unconditional annual mean and b) 99th percentile of daily accumulated precipitation (in mm/day) during the period from 2001 to 2012 over Congo by the 3B42_v7.0 product from 1°/daily FROGS database.

assessed considering the 3B42_v7.0 product as baseline. Overall, three different precipitation regimes, which were associated with the geographic characteristics, were observed across the five sub-basins of the Congo, which is in agreement with previous findings based on both the satellite and rain gauge data (e.g., Munzimi et al., 2015): i) Kasai and Luabala, located in the southernmost portion, presenting a well-defined dry/wet period, with the maximum (minimum) from November to March (between June and August); ii) Sangha and Ubangi, in the northern portions, presents a prolonged rainy period (peak of maximums around August/September) and a short-term dry season (December and January); and iii) the central part, which is characterized by a less well-defined monsoonal regime, with a dry period less pronounced and two rainy peaks (the first around March and the second during October/November).

Although all the satellite precipitation products were able to successfully represent the annual cycle of rainfall over each watershed under study, notable differences along the year on the magnitudes of the precipitation amounts were observed. Overall, two remarkable performance characteristics were noted. The group of satellite-only products mostly overestimates the rainy seasons' peaks compared to the rest of the products. In particular, the CMORPH_v1.0_RAW, 3B42RT_UNCAL_v7.0, followed by IMERG_V06_EU and IMERG_V06_LU products stand out for presenting the highest peaks, especially during the rainy seasons, systematically for all the five sub-basins. For instance, CMORPH_v1.0_RAW overestimates about 100 mm/month, in comparison to the rest of the products, at most of the sub-basins. On the other hand, the group of gauge-adjusted satellite products presented better agreements between each other and compared to 3B42_v7.0, except for GSMAP-gauges-RNLv6.0 and CMORPH_v1.0_CRT, which exhibited opposite performances to its satellite-only versions, underestimating the monthly totals during a greater part of the year for all the five sub-basins. In addition, TAMSAT_v2 stands out due to its difficulties in following the annual cycle properly (e.g., Central), underestimating the rainiest months at all sub-basins and also overestimating drier periods, especially over the northern portions (i.e., at Sangha and Ubangi).

Other particular basin characteristics and the performance diversities of both the satellite-only and gauge-adjusted products are clear considering the relative differences (%) of each product compared to 3B42_v7.0 as reference (in Supplementary Material, Fig. S1). The overestimations found by satellite-only products were relatively larger during the dry and dry-to-wet periods over Kasai and Luabala sub-basins. In this case, during these periods at Luabala, the 3B42_IR_v7.0, 3B42RT_UNCAL_v7.0 and CMORPH_v1.0_RAW products stand out for presenting the largest relative differences among all the sub-basins, with more than 300%, 200% and about

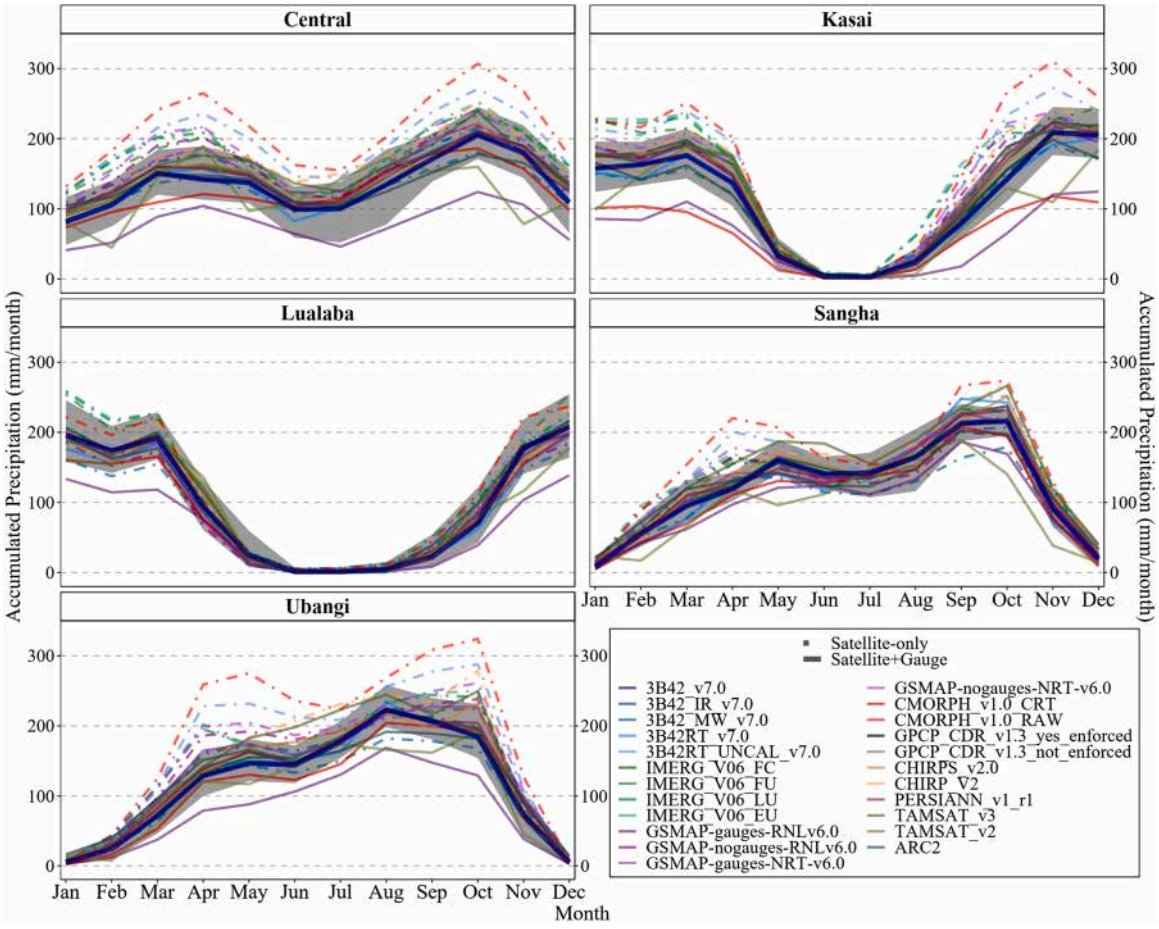

Fig. 3. Annual cycle of precipitation (in mm/month) during the period from 2001 to 2012 over the five Congo sub-basins from FROGs database. Dots and lines represent the monthly accumulated medians of each satellite-based precipitation product. Gray shading indicates the 30th and 70th percentile ranges. Satellite-only (gauge-calibrated satellite) precipitation products are represented by dashed (solid) lines.

290%, respectively. An opposite behavior, with negative relative differences (in about −100%) during the dry period at Kasai and Luabala sub-basins, was observed for the gauge-adjusted satellite group, with a slight exception; 3B42RT_v7.0 and CMORPH_v1.0_CRT (at Luabala). The regional TAMSAT_v2.0, TAMSAT_v3.0 and ARC2 products, in comparison to 3B42_v7.0 product, tend to overestimate January's amounts of precipitation (the dry period) at Sangha and Ubangi, which are consistent with the findings of Ayehu et al. (2018) for another African region.

It is worth mentioning that the performance and/or agreement of certain satellite precipitation products, in particular the native versions (satellite-only) and those ones adjusted/calibrated by rain gauges, in representing the local and/or regional precipitation regimes, are extremely linked to the region of interest. This is because the precipitation regimes are driven by multiple factors, including the frequency and intensity of rainy/non-rainy days to its monthly totals, as well as the contribution of a certain class of precipitation occurrences and the corroboration of moderate-extreme and extreme events over tropical land regions (Roca, 2019). These factors can be represented differently by satellite estimates and the differences are related to distinct aspects (e.g., the product technique itself, platform sources, gauge-adjustments, systematic uncertainties, among others).

The analyses were carried out by assessing the abilities of the satellite-based products in representing regionally, (for the five Congo watersheds), the mean annual cycle of precipitation distributions, which are controlled by the daily precipitation amount and occurrence contributions. Thus, the annual cycle of precipitation biases is then a consequence of the representation of the precipitation intensities, both in terms of occurrences and amounts (Gosset et al., 2018). According to Casse et al. (2015), the ability to reproduce the frequency distribution of rain rates and their contribution to the rainfall total are important criteria for hydrological applications, especially due to the impact of rainfall intensity, for instance, to the runoff. To assess how the precipitation amounts and occurrences are distributed according to the intensity scale, we looked at the cumulative density functions (CDF) of occurrence and volume (amount) of daily precipitation during the period from 2001 to 2012 over the five Congo sub-basins computed for each precipitation product (satellite-only and satellite gauge-adjusted) acquired from FROGs database. Through the CDF analysis, the relative contribution of each rain rate bin to the total rainfall volume and to the total number of occurrences can be assessed accordingly. We consider a logarithmically spaced precipitation bins, excluding the "zeros" (non-raining days). The analysis is performed per watershed and satellite-based precipitation product (separated per satellite-only and satellite gauge-adjusted categories), taking into account the entire period of sampling; from 2001 to 2012.

Fig. 4 shows the cumulative density functions of occurrence and volume (amount) of daily precipitation during the period from

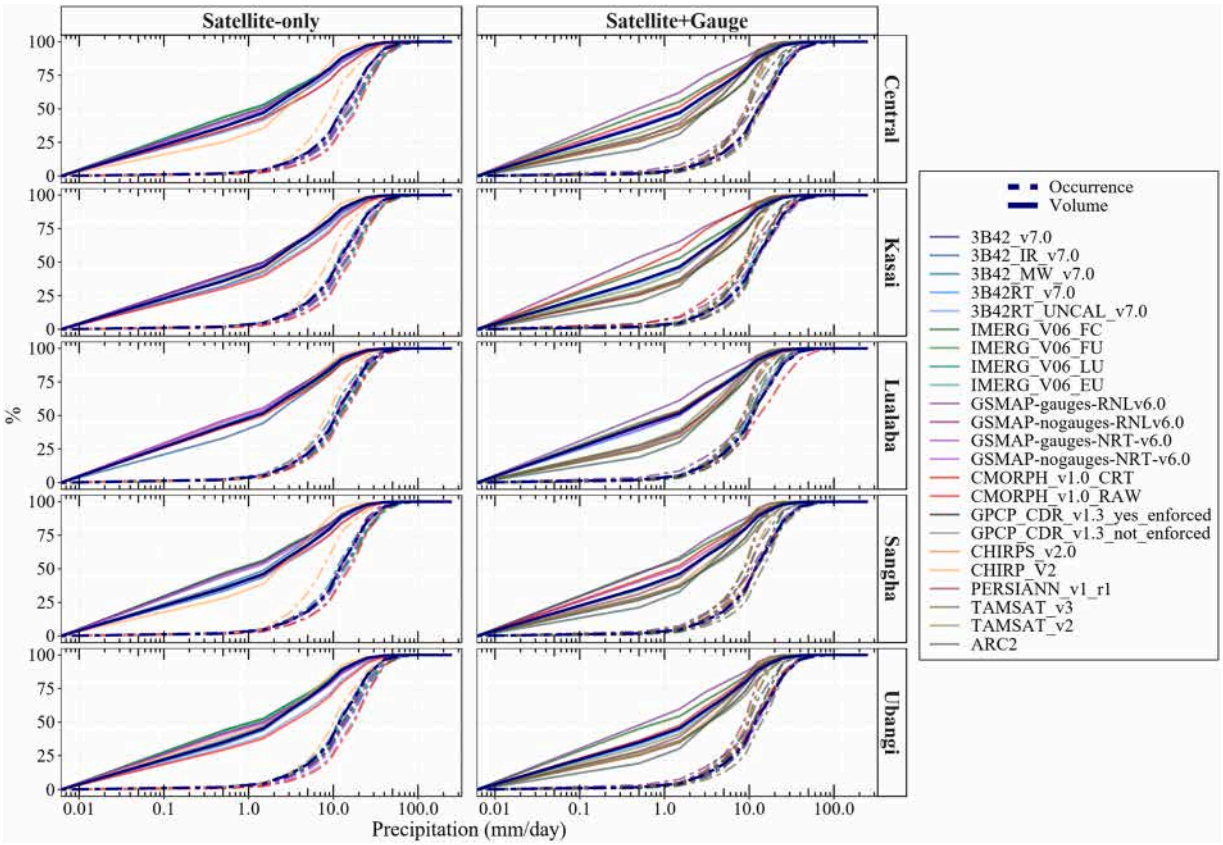

Fig. 4. Cumulative probability density functions of occurrence (dashed lines) and amount (solid lines) of daily precipitation during the period from 2001 to 2012 over the five Congo sub-basins from FROGs database. Satellite-only (gauge-calibrated satellite) precipitation products are represented at left (right) panels.

2001 to 2012 over the five Congo sub-basins computed for each satellite precipitation product (satellite-only and satellite gauge-adjusted) acquired from FROGs database. Through the overall CDF analyses, it becomes more evident, the differences between the two groups of satellite precipitation compared to the 3B42_v7.0 reference database. It is also possible to note that, even though the

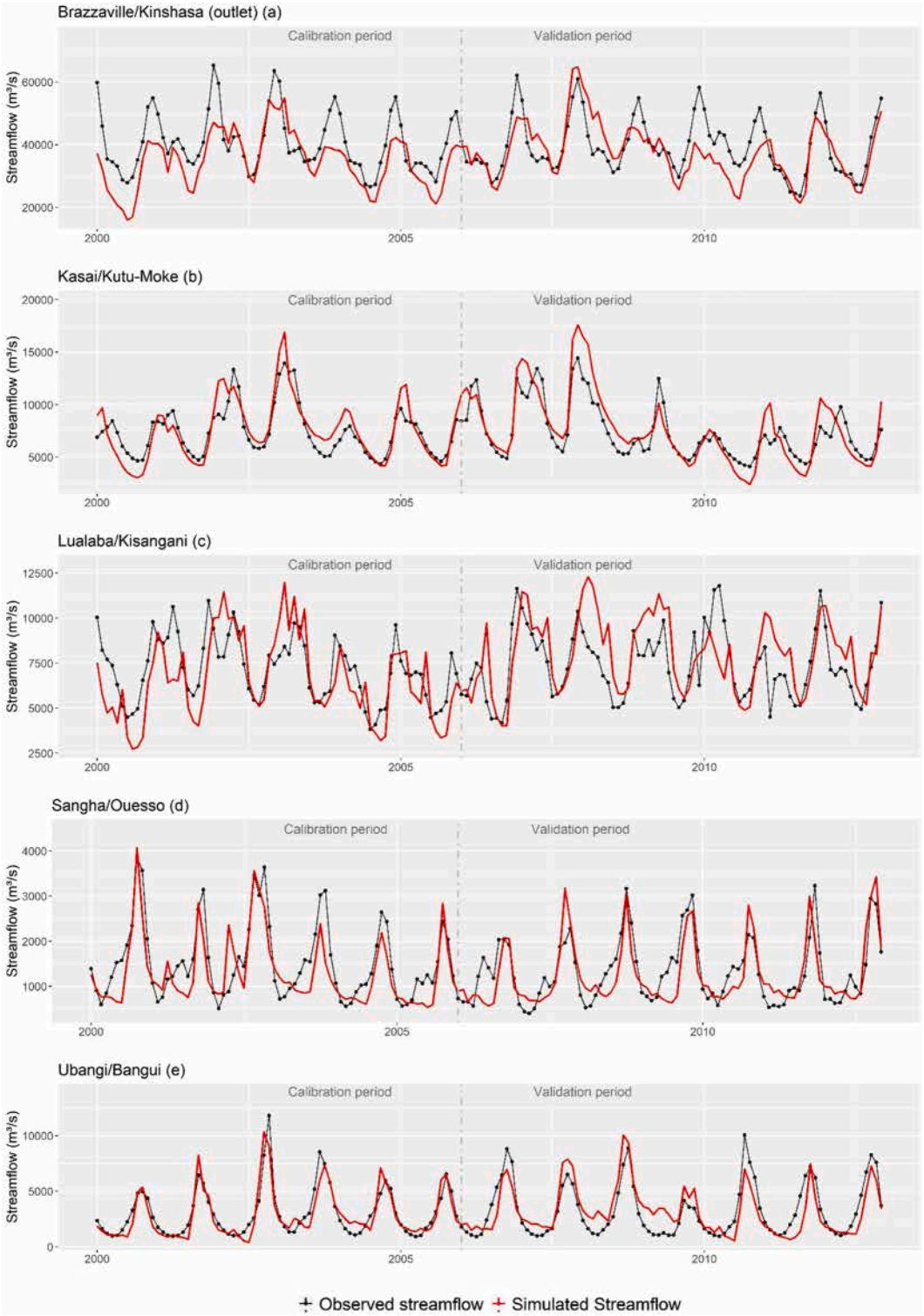

Fig. 5. Monthly observed and simulated streamflow at gauge stations (a) Brazzaville/Kinshasa (outlet), (b) Lualaba/Kisangani, (c) Kasai/Kutu-Moke, (d) Sangha/Ouesso, and (e) Ubangi/Bangui.

monthly totals are impacted differently, these two distinct CDF distributions are preserved for all the five watersheds. Better agreements between all the satellite-only products compared to the 3B42_v7.0, in both the occurrences and amounts of precipitation distributions, were observed. Slight overestimations (underestimations) on the amounts (occurrences) and frequencies of rainfalls lower (greater) than ~5 mm day^{-1} were observed from most of the satellite-only products compared to 3B42_v7.0. However, the ARC2 and CHIRP_V2 products presented opposite features, especially at the Luabala and the Central basins respectively. In contrast, the group of gauge-adjusted satellite precipitation products showed larger differences (heterogeneities) across all precipitation distribution ranges, especially in the volume of precipitation frequencies (e.g., up to 45% of frequency differences at precipitation intensities from 1 to 5 mm day^{-1}). In parallel to the scattered frequency distributions on the rainfall occurrences, an overestimation, most prominent at rainfall intensities greater than 10 mm day^{-}1, were observed from almost all the satellite+gauge products in comparison to 3B42_v7.0, except for CMORPH_v1.0_CRT (at Luabala) and TAMSAT_v2 (at Sangha and Ubangi). Such characteristics suggest that the gauge inclusion and/or adjustment techniques could directly impact quantitatively and qualitatively the daily precipitation distributions, from low to larger intensities, modifying its amount and occurrence frequencies.

3.2. SWAT model performance

3.2.1. Model calibration

The model was calibrated at a monthly time step at the outlet of the four main drainage units as well as the principal CRB outlet (Fig. 1). Table 3 summarizes the revised range of parameter values used in the calibration. Most of the parameters used to establish the model were groundwater parameters that have a strong influence on the water retention and transfer between the soil and aquifer. These parameters are within the limits of physically meaningful values indicated by Whittaker et al.(2010), Neitsch et al. (2011) and Pagliero et al. (2014) for the SWAT model. Calibrated values for the canopy storage parameter CANMX were defined for each crop. CANMX depends on the leaf area index of specific crops of which the evergreen forest has the highest value. For the parameters CH_N2 and CH_N1 that control channel roughness, we use the ranges recommended by Chow (1959).

3.2.2. Model efficiency

The simulated streamflow (Q_{sim}) matched the measured streamflow (Q_{obs}) and was synchronised with the variability in precipitation data for all gauge sites, for both calibration and validation periods (Fig. 5 and Table 4). The NSE, R^2 and KGE values for the calibration and validation periods for Ubangi/Bangui and Sangha/Ouesso gauges suggest good model performance. For Kasai/Kutu-Moke and Brazzaville/Kinshasa (outlet) gauges, these values suggest acceptable model performance, but for Lualaba/Kisangani the model, performance is less acceptable. The Ubangui and Sangha basins, mostly draining the northern hemisphere, present few hydrological and hydraulic singularities, thus it is not surprising that the conversion of rainfall into discharge is well performed by the model. The Lualaba sub-basin presents many lakes and swamps, including the Tanganyika lake whose behavior was complicated to model due to the lack of hydraulic / hydrological data (e.g. volume of water stored, surface area) for these lakes. PBIAS suggests a good fit between simulated and observed streamflow for all gauge sites. However, the PBIAS indicated an underestimation for the calibration period, except for Kasai/Kutu-Moke gauge; and overestimation for the validation period, with the exception of the Brazzaville/Kinshasa (outlet) gauge. (Table 5).

Fig. 6 shows the relative error between Q_{obs} and Q_{sim} (positive values indicate overestimated Q_{sim} and negative values indicate underestimated Q_{sim}). For Ubangi/Bangui, Sangha/Ouesso, and Kasai/Kutu-Moke, the model in general overestimated low flows in Q_{obs} in the calibration and validation periods. Conversely, for Lualaba/Kisangani and Brazzaville/Kinshasa (outlet) the model underestimated low flows periods. The peak flow at Brazzaville/Kinshasa (outlet) was underestimated, while for other gauges the peak flow was slightly underestimated. The overestimation of minimum values of Q_{obs} is linked to the lower baseflow and faster recession during the dry season. This overestimation could not be corrected by an increase of baseflow recession constant, because it would lead to overestimating streamflow during the beginning of the rainy season. Further details about the drainage sub-basins and calibration and validation can be found in Datok et al. (2022).

Model performance results shown in this section depend on the design and assumptions of the SWAT model and represent one example of an application of this model in the CRB. The SWAT model was originally developed for temperate zones, which means that input data and the calibration method needs to be improved for tropical basins (Wagner et al., 2011; Strauch and Volk, 2013; Alemayehu et al., 2017; Dos Santos et al., 2018). Different modifications have been made to the classic SWAT model including the addition of different variations of wetland and reservoir modules (Liu et al., 2008; Sun et al., 2015; Guilhen et al., 2020). However, they still have their shortcomings, including the need for more data, and a lack of a proper representation of physical processes (Phiri et al.,

Table 4
SWAT model performance for predicting monthly streamflow.

	Calibration				Validation			
	NSE	R^2	PBIAS	KGE	NSE	R^2	PBIAS	KGE
Brazzaville/Kinshasa (outlet)	0.16	0.59	14.52	0.71	0.44	0.54	4.10	0.71
Kasai/Kutu-Moke	0.63	0.76	-2.11	0.48	0.59	0.78	-4.66	0.48
Lualaba/Kisangani	0.02	0.49	7.84	0.23	0.08	0.39	-8.19	0.23
Sangha/Ouesso	0.67	0.71	8.37	0.80	0.59	0.65	-1.30	0.80
Ubangi/Bangui	0.81	0.83	4.01	0.90	0.66	0.67	-0.86	0.90

Table 5
Summary of various hydrological studies utilizing satellite-based precipitation products run with the SWAT model.

Satellite-based precipitation products	Period	Study area	Latitude	Recalibration of parameters	Highlight	Reference
3B42_v7.0 and CHIRPS_v2.0	1998 – 2010	Adige Basin (Italy)	45°N	yes	Four precipitation datasets were tested, where two were satellite-based. The satellite dataset was compared to data from de precipitation gauge stations. The results indicate the applied precipitation input influenced the estimated model parameters.	Tuo et al. (2016)
IMERG_v6.0_EU, IMERG_v6.0_LU and IMERG_v6.0_FC	2014 – 2016	Kelantan Basin (Malaysia)	6°N - 4°N	yes	The satellite dataset was compared to data from de precipitation gauge stations. IMERG_FC outperformed the near real-time products in cumulative streamflow measurement. The results indicate the IMERG products could be an alternative precipitation source for this region.	Tan et al. (2018)
3B42_v7.0 and IMERG_v6.0_FC	2000 – 2018	Tocantins-Araguaia basin (Brazil)	14°S – 16°S	yes	Two satellite-based precipitation products were tested. The satellite dataset was compared to data from de precipitation gauge stations. The results demonstrating the satellite dataset were able to simulate the hydrological regime adequately.	Amorim et al. (2020)
3B42_v7.0 and CHIRPS_v2.0	2001–2012	Gurupura basin (India)	13°N – 12°N	yes	Tree precipitation datasets were tested, where two were satellite-based. CHIRPS has been tested with two different resolutions: 0.05 and 0.25. 3B42_v7.0 performed better than CHIRPS-0.05, and CHIRPS-0.25, but 3B42_v7.0 underestimated the flow for agricultural water availability in 30%.	Sharannya et al. (2020)
PERSIANN-CDR_v1_r1, CHIRPS_v2.0, CMORPH_IFlOODS_v1.0, IMERG_v6.0_FC, GSMaP_gauges_v6. and 3B42_v7.0	1998–2019	Tarim Basin (China)	41°N	no	Seven satellite-based precipitation products were tested. The satellite dataset was compared to data from de precipitation gauge stations. The IMERG_v6.0_FC and PERSIANN-CDR_v1_r1were the best datasets for the daily and monthly scale precipitation accuracy evaluations. PERSIANN-CDR_v1_r1 and CMORPH_IFlOODS_v1.0 performed better than others in monthly runoff simulations. All datasets have the potential to provide valuable input data in hydrological modeling.	Peng et al. (2021)
CHIRPS_v2.0, 3B42_v7.0, CMORPH_CRT and PERSIANN-CDR_v1_r1	1998–2014	Ganjiang Basin (China)	28°N – 24°N	no	Four satellite-based precipitation products were tested. The satellite dataset was compared to data from de precipitation gauge stations. The results indicate 3B42_v7.0 provides the most accurate hydrological model simulation results, while simulated streamflow forced by CMORPH_CRT exhibits considerable underestimation of streamflow.	Wang et al. (2021)

2021). Input variables that are associated with the wetlands include the surface areas and volumes of water at normal and overflowing, as well as the fraction of the subbasin area draining into the wetland. The absence of these data as well as the quality and resolution of the DEM add to the uncertainties of the model. The PBIAS however suggests a good fit between the simulations and observations. The timing of flood events, the bimodal pattern of rainfall over the basin, wet and dry years and also the regularity of groundwater flow over the simulation period were well captured. The results from the Datok et al., 2020 model, also hint at a hydrological disconnect of

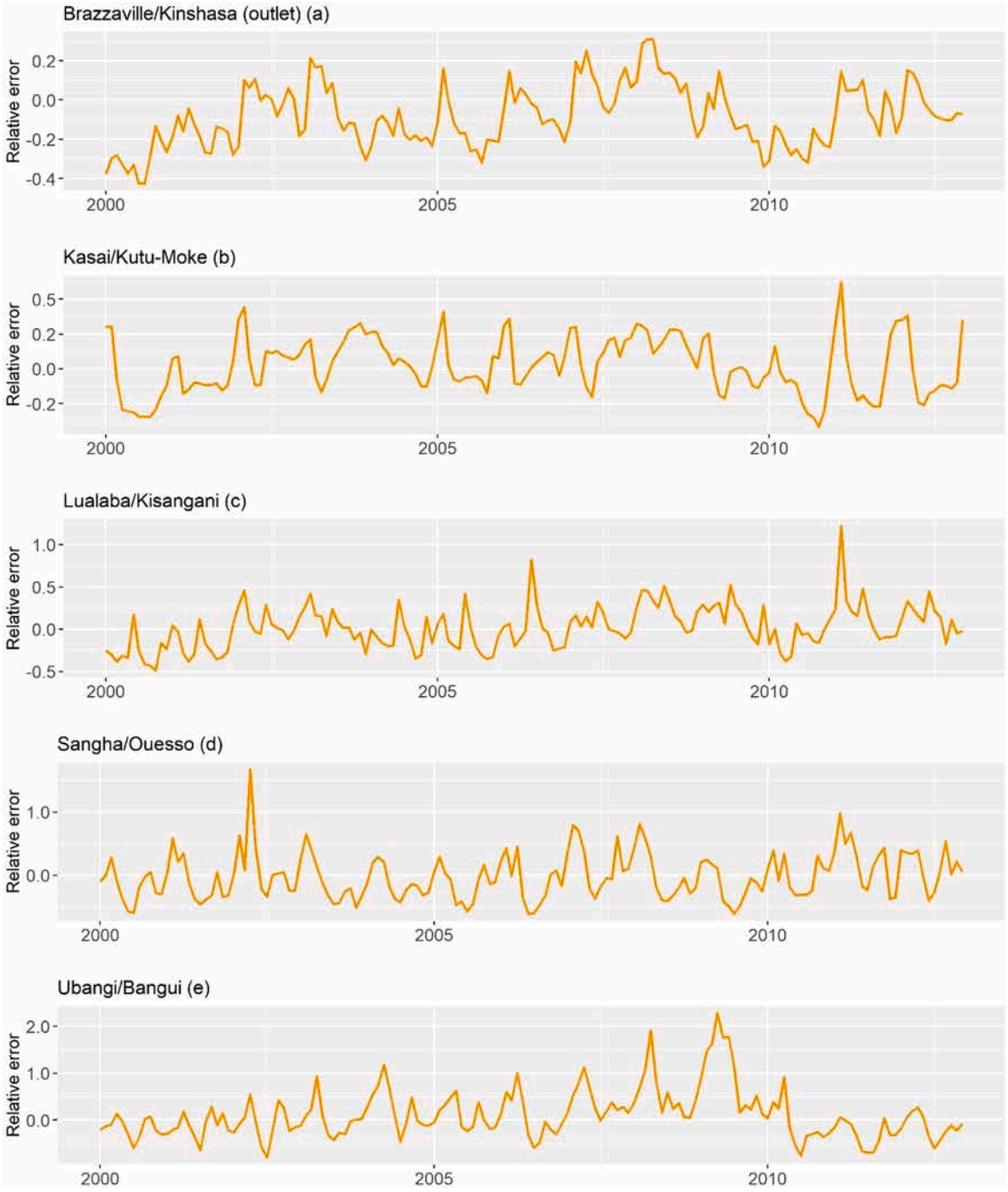

Fig. 6. Relative error between observed and simulated streamflow (Relative error = $(Q_{sim} - Q_{obs})/Q_{obs}$) at gauge stations (a) Brazzaville/Kinshasa (outlet), (b) Lualaba/Kisangani, (c) Kasai/Kutu-Moke, (d) Sangha/Ouesso, and (e) Ubangi/Bangui.

the upper Congo with the drainage basin due to the presence of natural reservoirs, which cause significant lag. This result is in conformity with the work of Kitambo et al., 2021, in which similar observations with respect to surface water extent and height were considered.

Similar to the results from Kitambo et al., 2021, the Datok et al. (2022) model shows surface runoff start to increase around April to May and reach maximum levels from October-November in the northern tributaries. This result shows that inspite of the weak correlation in the Lualaba basin, much like in Kitambo et al., 2021, the results at the basin outlet at Brazzaville/Kinshasa are not strongly influenced by this subbasin. Therefore, the contribution of the upper Congo to the discharge of flow and sediments to the basin outlet are negligible, and since this particular region presents the highest level of uncertainty in our calibrated model, it gives us a higher

degree of confidence in our model outputs.

In addition, there is a generally good agreement between simulation and observation of hydrological parameters like rainfall, evapotranspiration, seasonality and discharge in a majority of the model subbasins, and less acceptable ones in other regions (Datok et al., 2022). Therefore, this study adds to the argument that the benchmarks used for the performance metrics should be hydrologically meaningful and hence subjective, by taking into account the objectives of the study, the available observations, and parameter values (Knoben et al., 2019).

3.3. Hydrological evaluation

3.3.1. Streamflow

The hydrographs (Fig. 7) indicate that the SWAT model follows the key features of the satellite precipitation products as the dry and wet season at the five-gauge sites studied show. Thus, it is possible to evaluate the performance of those products without recalibration. It is expected however that the twenty-two precipitation product inputs lead to different streamflow prediction than the 3B42_v7.0 (base scenario) at all five-gauges. In general, and as expected, the products without precipitation adjustments (satellite-only) predicts higher streamflow. However, according to the results some satellite products behave differently, for example CMORPH_v1.0_CRT predicts higher streamflow at the gauge Lualaba/Kisangani, but in other gauges, this product underestimated the streamflow.

Statistical analysis (Fig. 8) and the Δ% (Supplementary Material—Table S2) demonstrated that the hydrological model driven by the precipitation products with precipitation adjustments (satellite+gauge) performed better than those without precipitation adjustments; as expected, but trends between the products and differences between the regions are evident. The KGE and PBIAS indexes indicates some products can provide satisfactory performance at Ubangi/Bangui, Lualaba/Kisangani and Brazzaville/Kinshasa (outlet) without model recalibration. Fig. 8 also highlights that the GPCP_CDR_v1.3_not_enforced, which is a satellite only product,

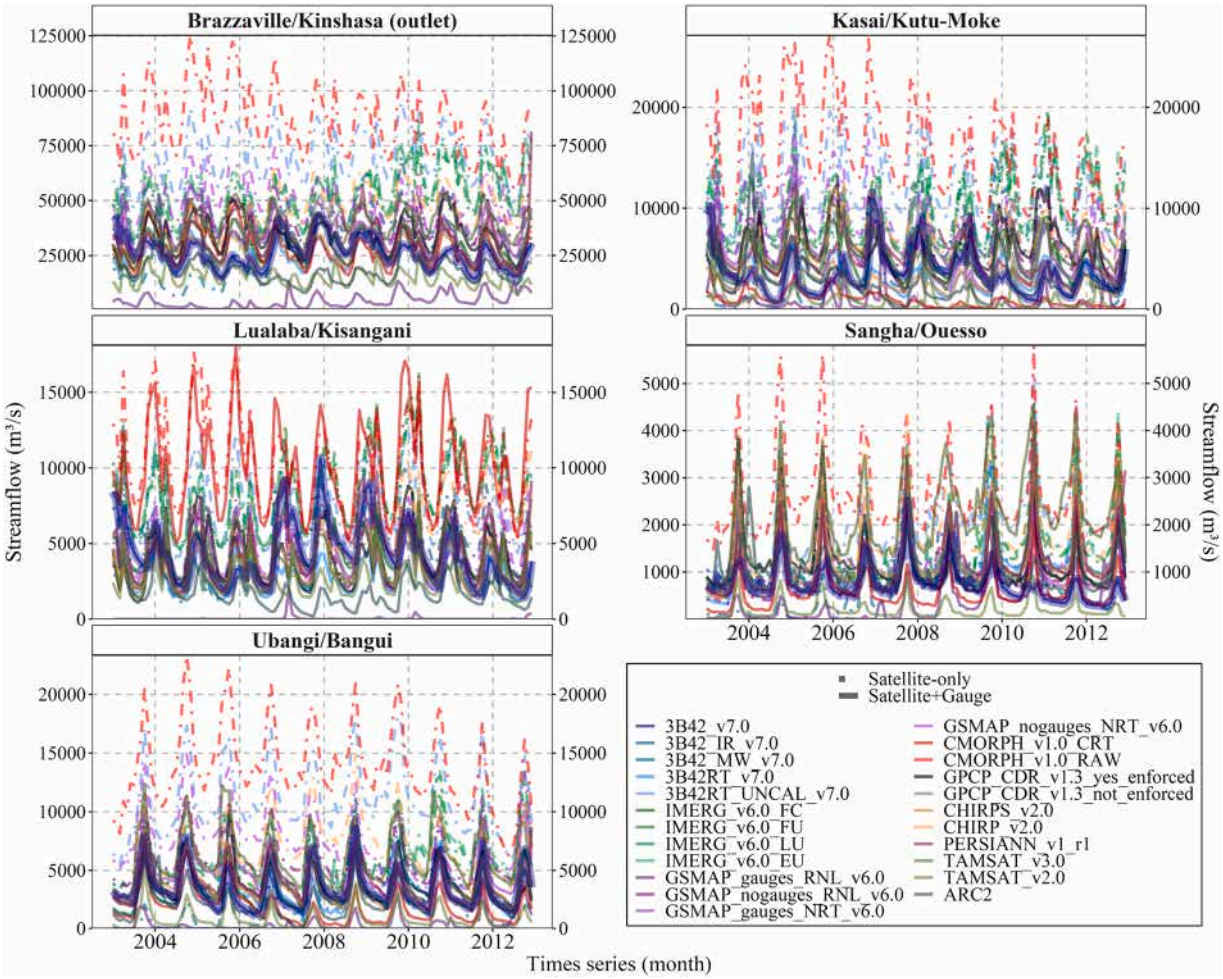

Fig. 7. Simulated streamflow (in m^3/s) hydrographs during the period from 2003–2012 for gauges stations: Brazzaville/Kinshasa (outlet), Kasai/Kutu-Moke, Lualaba/Kisangani, Sangha/Ouesso and Ubangi/Bangui. Dots and Lines represent the monthly streamflow of each satellite-based precipitation product. Satellite-only (gauge-calibrated satellite) precipitation products are represented by dashed (solid) lines.

demonstrates a good performance (KGE 0.71) at Ubangi/Bangui gauge. When looking at the entire CRB, the worst scores were obtained by 3B42RT_UNCAL_v7.0 and CMORPH_v1.0_RAW satellite-only products. It is evidenced by Fig. 8 that while some satellite-only products tend to lead to higher streamflow predictions (such as CMORPH_v1.0_RAW and 3B42RT_UNCAL_v7.0), others as 3B42_IR_v7.0 and 3B42_MW_v7.0 tend to lead to lower streamflows in particularl at Sangha/Ouesso and Ubangi/Bangui dry regions of CRB. The regional products (TAMSAT v2.0, v3.0 and ARC2) did not perform well in estimating streamflow, when compared to quasi-global products such as the IMERG_v6.0_FC or land-only products like the CHIRPS_v2.0. Although ARC2 performed better than the other regional products, it still underestimated the streamflow at four-gauge stations.

The near-real-time (NRT) precipitation products (important for now-casting and forecasting streamflow in applications such as early warning systems) such as IMERG_v6.0_EU and IMERG_v6.0_LU did not provide a good prediction of streamflow, showing a consequent overestimation at all gauges. Among the NRT products, only 3B42RT_v7.0 had a good performance at the Ubangi/Bangui stations, and Brazzaville/Kinshasa (outlet) and Kasai/Kutu-Moke. The PBIAS indicates a good performance when compared to the base scenario, maybe due to the similarities with the product used in our base scenario.

In general, the monthly streamflow simulation results and the statistical scores from IMERG_v6.0_FC and CHIRPS_v2.0 presented consistent streamflow simulations, except for Kasai/Kutu-Moke and Sangha/Ouesso gauges. Studies as Tan et al. (2018) and Amorim et al. (2020) have shown the better performance of IMERG products to estimate streamflow all around the world in comparison to TMPA products, due to its improvement in precipitation estimation. In our case, the recalibration of model parameters for IMERG products could improve streamflow simulations, specifically at the gauge stations where 3B42_v7.0 did not perform well.

3.3.2. Water balance components

To better understand the influence of the different precipitation products in predicting the water balance components (WBC) utilizing the SWAT model, we analyzed the monthly cycle of evapotranspiration (ET), surface runoff (SURQ), lateral flow (LATQ), percolation (PERC), soil water content (SW), groundwater contribution to streamflow (GWQ) and water yield (WYLD) simulated at the sub-basin scale. The results show that the satellite-only products tend to overestimate the WBC, especially in the rainy season. However, the level of overestimation and underestimation depends on the type of WBC and the region in the CRB.

For ET predictions (Fig. 9), the precipitation products have the tendency to overestimate in both dry and wet seasons when compared to 3B42_v7.0, although some track ET much more closely than others. The CMORPH_v1.0_RAW and GSMAP_gauges_RNL_v6.0 have the tendency to underestimate this component. Peak basin-wide ET during March is overestimated for almost all products, while the basin's low at June, July and August is underestimated at Lualaba and overestimated at other regions. At Ubangi, most of the precipitation products capture the same tendency of 3B42_v7.0 between June to February. Overall, the global ET prediction is overestimated at all sub-basins (in Supplementary Material, Table S3).

The SURQ (Fig. 10), LATQ and PERC (Supplementary Material - Figs. S4 and S5) predictions -which are intrinsically linked to the amount and dynamics of precipitation- are similar for the dry season at Kasai, Ubangi and Sangha sub-basins. However, none of the products capture the full amplitude of fluctuations across seasons at the Central and Lualaba sub-basins. The predictions are

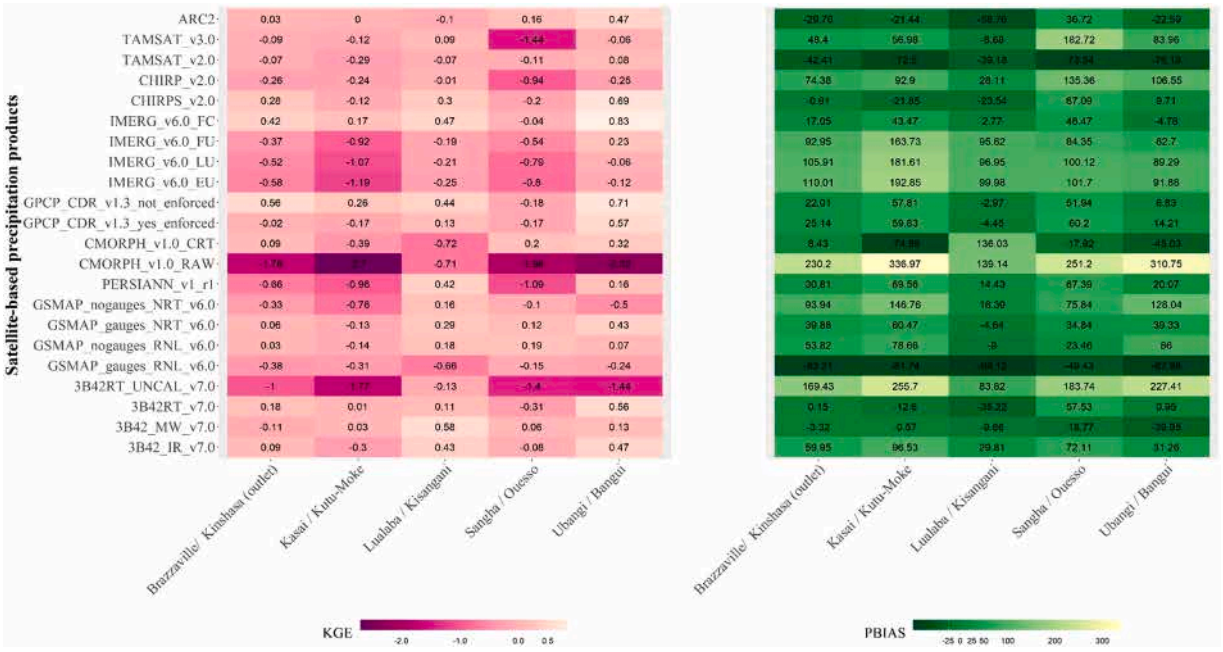

Fig. 8. Heat map statistical analysis (KGE and PBIAS) of the streamflow simulation results of the selected satellite-based precipitation product. The statistical analysis was calculated using the streamflow from base scenario (3B42_v7.0) as reference.

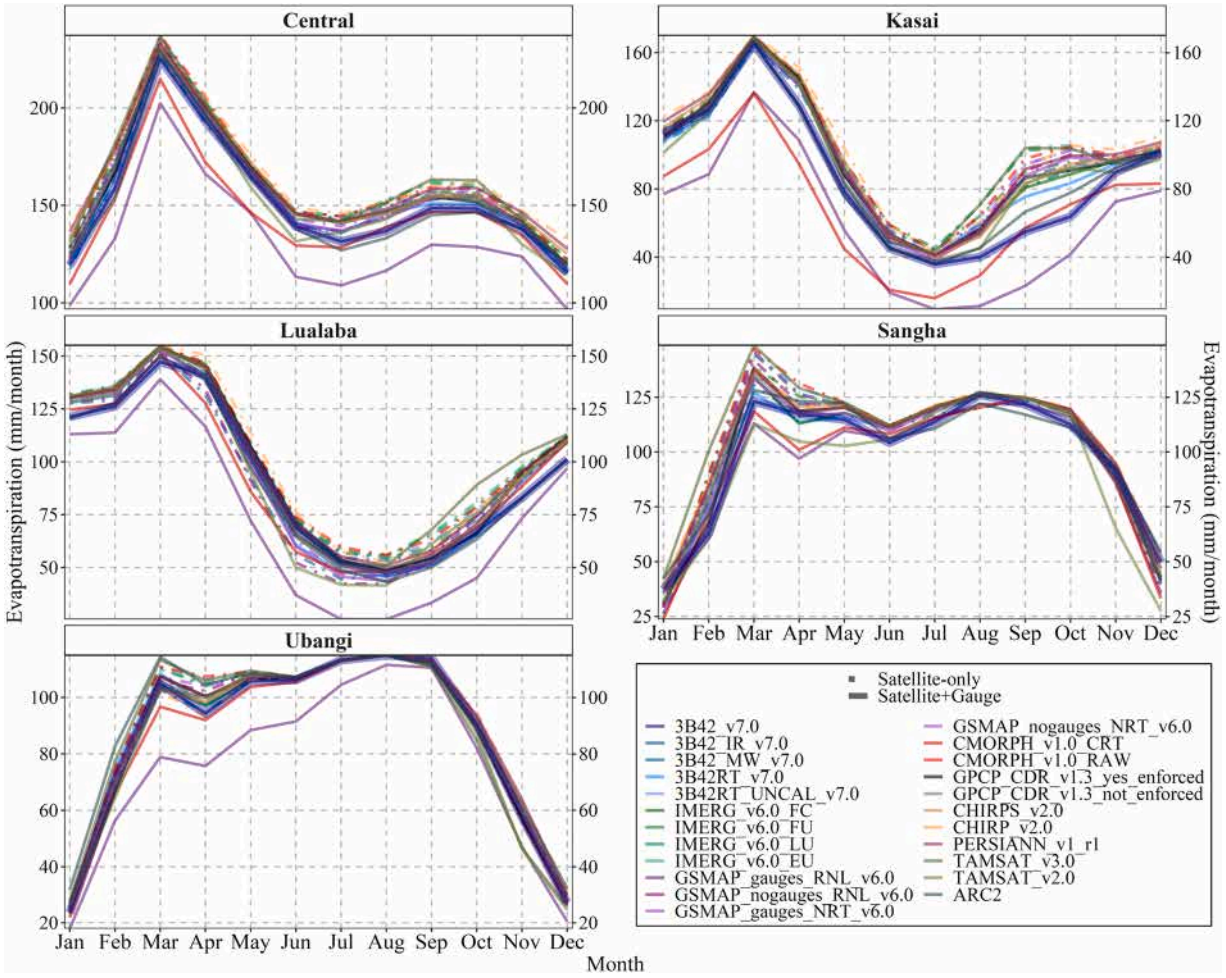

Fig. 9. Simulated annual cycle of evapotranspiration (in mm/month) during the period from 2003 to 2012. Dots and lines represent the monthly accumulated medians of each satellite-based precipitation product. Satellite-only (gauge-calibrated satellite) precipitation products are represented by dashed (solid) lines.

overestimated even in the dry season. For the wet season, the satellite precipitation products have the tendency to overestimate these components in regards to 3B42_v7.0 at five regions. Kasai and Lualaba sub-basins presenting one large peak of SURQ, LAT and PERC between November to March. Sangha and Ubangi have one peak around August/September while the Central region has two peaks, the first around March/April and the second during October/November. These peaks are overestimated and some products as TAMSAT_v3.0 and ARC2 do not follow the same seasonal shape of 3B42_v7.0. In general, the global SURQ, LATQ and PERC (in Supplementary Material, Table S3) are overestimated, although some track much more closely than others, especially in the dry season.

The SW (Fig. 11) and GWQ (Supplementary Material - Fig. S6) predictions, - which refers to water stored in soil - demonstrate a wide range of simulated values, particularly for GWQ, hence overestimateing these components for both satellite-only and satellite+gauge with respect to 3B42_v7.0. For SW, the precipitation products generally follow the seasonal shape, except some products as CMORPH_v1.0_RAW and GSMAP_gauges_RNL_v6.0 although none of them capture the full amplitude of fluctuations across seasons. The tracks are closer than others for SW in the dry season at Lualaba and Ubangi, but for Central, Kasai and Sangha, the tracks are scattered.

The seasonal cycle of GWQ does not present a large fluctuation across seasons, but the tracks are scattered at all regions studied. This behaviour could be linked to the SWAT model, because the model simulates groundwater using the two-way groundwater-surface water exchange which limits the ability to predict groundwater storage (Shao et al., 2018, Melaku and Wang, 2019). Also, the surface water-groundwater interaction mechanisms are less studied than other WBC in the Congo Basin (Alsdorf et al., 2016).

The WYLD (Supplementary Material—Figures – S6) predictions (consisting of: surface runoff + groundwater flow + tile flow − transmission loss) are also overestimated compared to 3B42_v7.0. The peak flows have the same characteristic of SURQ at all regions, with two peaks at the Central, Kasai and Lualaba. However, peak shapes of some precipitation products are wider than the peak of 3B42_v7.0. Similar to the GWQ, the WYLD tracks are scattered at all sub-basins.

Overall, the trends between the precipitation products and differences between the regions affects the WBC. The Δ%

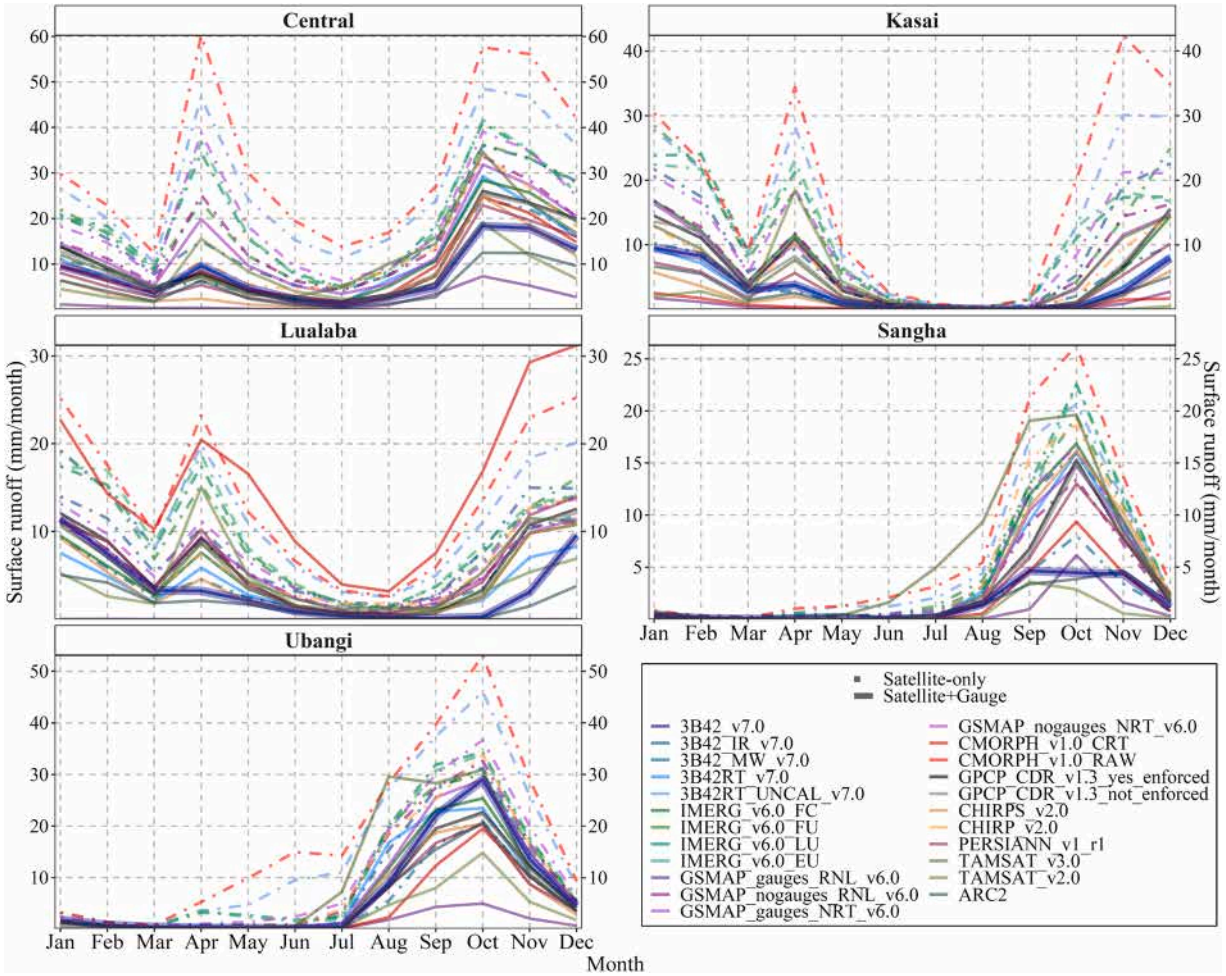

Fig. 10. Simulated annual cycle of surface runoff (in mm/month) during the period from 2003 to 2012. Dots and lines represent the monthly accumulated medians of each satellite-based precipitation product. Satellite-only (gauge-calibrated satellite) precipitation products are represented by dashed (solid) lines.

(Supplementary Material—Table S3) showed that even a small increase or decrease of amounts of precipitation would cause increase or decrease in the WBC, especially the components that are dependent on the dynamics of precipitation as surface runoff and percolation. However, some precipitation products behave differently, for example, in most of the analyzed products, an increase in amount of precipitation leads to an increase in the values of the WBC, but CMORPH_v1.0_CRT shows a decrease of amount of precipitation then an increase in surface runoff values at the Central, Kasai and Sangha, that leads to a decrease of percolation. Several possible causes could lead to these results, the hydrological response of the WBC is linked to precipitation and design and assumptions of the model to type of vegetation, topography and soil. It is expected that in forest areas there will be less surface runoff than in pasture areas for example. Soil degradation will also lead to an increase of runoff.

3.4. Influence of the precipitation input on model performance

To compare the hydrological performance of the satellite-based precipitation products using the SWAT model, we summarized some recent hydrological evaluation studies around the world in Table 4 (Tuo et al., 2016; Tan et al., 2018; Amorim et al., 2020; Sharannya et al., 2020; Peng et al., 2021; Wang et al., 2021). Four main conclusions can be drawn from the comparisons: i) in many cases, the IMERG_v6.0_FC outperforms 3B42_v7.0 in hydrological simulations due to its improvement in precipitation estimation; ii) the performance of the satellite-based precipitation products depends on the basin localization and simulations scale (daily or monthly); iii) hydrological model choice will affect the accuracy assessment of precipitation products for detecting streamflow extremes; and iv) the recalibration of the model parameters for each satellite-based precipitation product effectively improved the precision of streamflow simulations.

As shown in the hydrological evaluation section, the IMERG_v6.0_FC and CHIRPS v2.0 products demonstrates good performance without recalibration and could be used to study the hydrological cycle in the CRB, especially for streamflow and evapotranspiration.

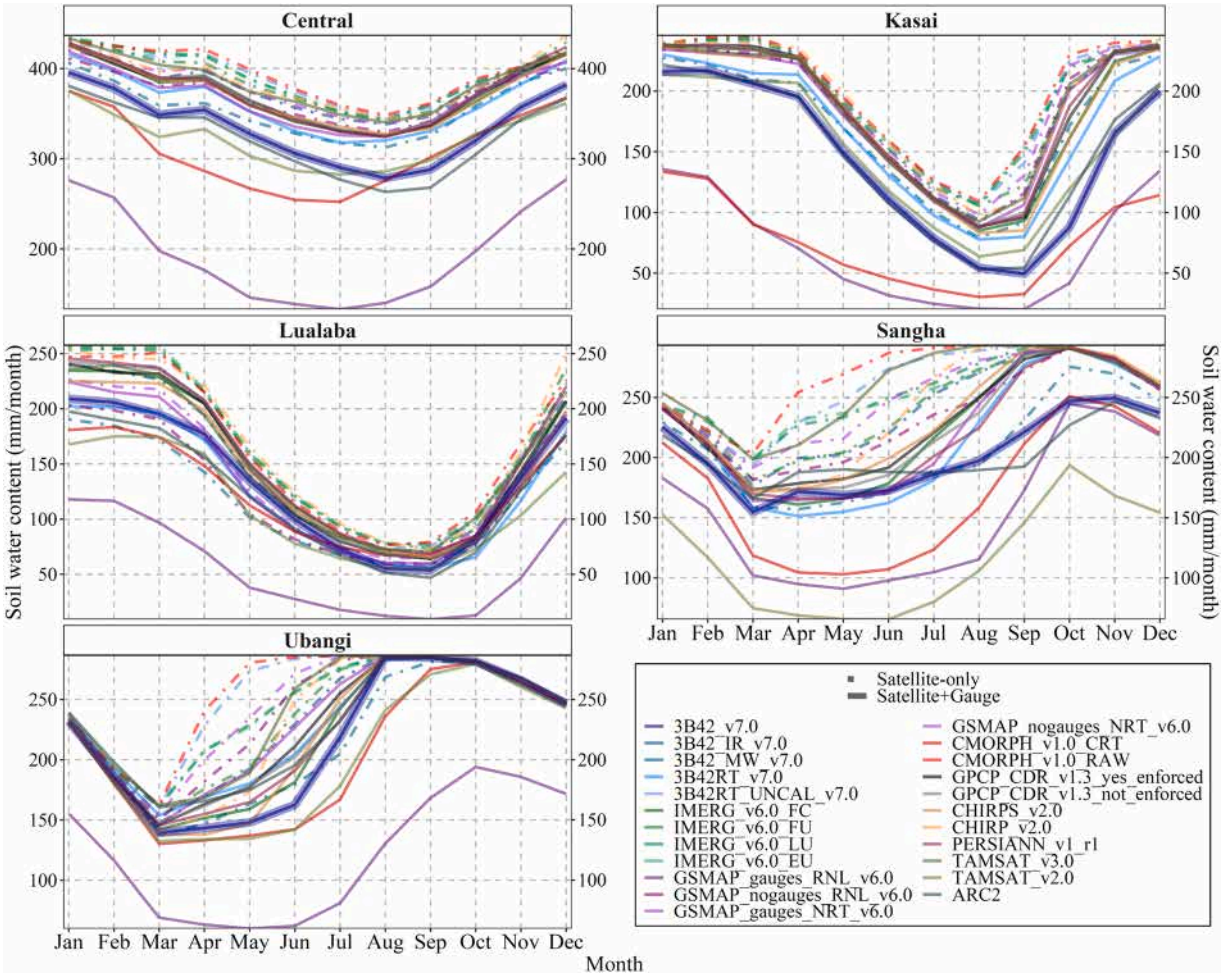

Fig. 11. Simulated annual cycle of soil water content (in mm/month) during the period from 2003 to 2012. Dots and lines represent the monthly accumulated medians of each satellite-based precipitation product. Satellite-only (gauge-calibrated satellite) precipitation products are represented by dashed (solid) lines.

These results agree with the findings reported in Table 4, and a recalibration of the model parameters could effectively improve the precision of satellite-based precipitation product simulations, especially for WBC that are connected to the amount and dynamics of precipitation as SURQ, LATQ and PERC.

Nevertheless, the bias in satellite-based precipitation products was recognized as a major issue across several basins around the world (Maggioni and Massari, 2018), and the inaccuracy of satellite data may lead to unrealistic parameter values when recalibrating the model (Peng et al., 2021). Maggioni and Massari (2018) have shown that model recalibration was also raised as a viable option to improve streamflow simulations from satellite-based precipitation products, but caution is necessary when recalibrating models. Another option is the bias correction of the satellite products with ground-based measurements of precipitation to obtain more realistic flow simulations (Wang et al., 2021).

CRB model calibration was based on a trial and error basis (see above). We ran the model several times using parameters calculated either from known physical information about the basin or from information obtained from literature and global datasets. We tried as much as possible to fix the parameters to be as realistic as possible, there is a chance that some of the hydrological behaviours of the system were not captured accurately (Datok et al., 2022). It is possible that the model recalibration for each precipitation product could improve the results, especially for streamflow. However TMPA 3B42 v.7 (reference subset) tends to underestimate rainfall in the CRB (Beighley et al., 2011; Munzimi et al., 2015). The precipitations products analyzed is this study, largely tend to overestimate the rainfall in the CRB (Fig. 3), which could lead to unrealistic parameters, especially those associated with the movement and storage of groundwater and also the runoff.

Numerous researchers have examined the quality of satellite derived precipitation datasets through hydrological modelling (e.g.: Beck et al., 2017, Dembélé et al., 2020). Beighley et al. (2011) analyzed the TRMM, CMORPH and PERSIANN dataset through the Hillslope River Routing (HRR) model in the CRB to predict streamflow and water storages, and some of their results are similar to ours. Notably, CMORPH tends to overestimate magnitudes and TRMM shows reasonable agreement relative to the historical observations.

However, PERSIANN performed better in capturing the pattern of streamflow in the SWAT model, having a performance close to 3B42_v7.0 (TRMM) (Supplementary Material - Tables S2 and S3). The different results may be linked to the design and assumptions of these two models or the PERSIANN bias correction carried out in recent years.

Satellites estimate appear not to perform well over the CRB (McCollum et al., 2000; Awange et al., 2016) and there are large discrepancies between gauge-based products from GPCC (Global Precipitation Climatology Centre), CMAP (CPC Merged Analysis of Precipitation), GPCP (Global Precipitation Climatology Project), and CPC (Climate Prediction Center) in the interannual and decadal variations in precipitation over the basin (Negron Juarez et al., 2009). The lack of a dense and reliable network of rain gauges makes it impossible to assess quantitatively, the rainfall products against a proper ground validation reference. In addition, for the long-term mean, GPCP and CMAP display the major precipitation patterns, although substantial discrepancies occur in areas with low gauge densities, such as equatorial West Africa (Yin et al., 2004). However, independent of these discrepancies, our findings show that the IMERG_v6.0_FC and CHIRPS v2.0 are potential alternative sources of data for hydrological modeling using SWAT in the CRB.

4. Conclusions

The present work investigated the performances of 23 satellite-based precipitation products (Table 1) in simulating streamflow and water balance components at the Congo River Basin through the SWAT model. The key findings are as follows:

The precipitation products were able to represent with consistency the annual cycle of rainfall and the frequencies of rain intensities/occurrences over each sub-basin studied. However, the precipitation amounts during the year are different, especially due to high precipitation intensities. In the absence of a reliable dense ground validation network, the gauge adjusted version of 3B42_v7.0, which has been shown to provide good simulations of the discharge through the SWAT model, was taken as a benchmark to analyze the skills of other precipitation products. Overall, the group of satellite-only precipitation products mostly overestimates the rainy season peaks; and the gauge-adjusted satellite products presented better agreements between each other and compared to 3B42_v7.0, except for GSMAP-gauges-RNLv6.0 and CMORPH_v1.0_CRT.

Streamflow and water balance components simulation replicate precipitation products patterns, and gauge-adjusted satellite performed better than satellite-only for streamflow. In addition, during the rainy season, the precipitation products have the tendency to overestimate the SURQ, LATQ and PERC in regards to 3B42_v7.0 over the Congo Basin. For other components (ET, SW, GWQ and WYLD) and streamflow predictions, there is an overestimation at all sub-basins. However, IMERG_v6.0_FC and CHIRPS v2.0 products demonstrate good performance with our model, and could be used to predict the hydrological cycle.

In general, the selection of precipitation products has a crucial effect on model performance and has to be taken into consideration since it is one of the sources of uncertainties. Unfortunately, the Congo River Basin is deprived of a quality and dense rain gauge network for assessing these uncertainties more quantitatively. Using the hydrological model with an ensemble of available products provides a good illustration of the impact of the uncertainties and can be used to filter out the products which behave like outliers and/or to indicate the confidence in the simulated hydrological variables. The combination of bias correction of the satellite products with ground-based measurements and recalibration of the model parameters could effectively improve predictions of the hydrological cycle.

Declaration of Competing Interest

The authors declare that they have no known competing financial interests or personal relationships that could have appeared to influence the work reported in this paper.

Acknowledgments

We thank the FUI (Fonds Unique Interministériel) HydroSIM project (2018–2021). We also thank the TETFUND, Nigeria for funding P. Datok stay at the Laboratoire Ecologie Fonctionnelle et Environnement, Université de Toulouse, France and finally to CNES-TOSCA for providing part of the funds for this research.

Appendix A. Supporting information

Supplementary data associated with this article can be found in the online version at doi:10.1016/j.ejrh.2022.101168.

References

Abbaspour, K.C., Rouholahnejad, E., Vaghefi, S., Srinivasan, R., Yang, H., Kløve, B.A., 2015. continental-scale hydrology and water quality model for Europe: calibration and uncertainty of a high-resolution large-scale SWAT model. J. Hydrol. 524, 733–752. https://doi.org/10.1016/j.jhydrol.2015.03.027.

Akoko, G., Le, T.H., Gomi, T., Kato, T., 2021. A review of SWAT model application in Africa. Water 13, 1313. https://doi.org/10.3390/w13091313.

Alemayehu, T., Van Griensven, A., Woldegiorgis, B.T., Bauwens, W., 2017. An improved SWAT vegetation growth module and its evaluation for four tropical ecosystems. Hydrol. Earth Syst. Sci. 21, 4449–4467. https://doi.org/10.5194/hess-21-4449-2017.

Aloysius, N., Saiers, J., 2017. Simulated hydrologic response to projected changes in precipitation and temperature in the Congo River basin. Hydrol. Earth Syst. Sci. 21, 4115–4130. https://doi.org/10.5194/hess-21-4115-2017.

Alsdorf, D., Beighley, E., Laraque, A., Lee, H., Tshimanga, R., O'Loughlin, F., Mahé, G., Dinga, B., Moukandi, G., Spencer, R.G.M., 2016. Opportunities for hydrologic research in the Congo Basin. Rev. Geophys. 54 (2), 378–409. https://doi.org/10.1002/2016RG000517.

Amorim, Jd.S., Viola, M.R., Junqueira, R., Oliveira, V.Ad, Mello, C.Rd, 2020. Evaluation of satellite precipitation products for hydrological modeling in the Brazilian Cerrado biome. Water 12 (9), 2571. https://doi.org/10.3390/w12092571.

Arnold, J.G., Srinivasan, R., Muttiah, R.S., Williams, J.R., 1998. Large area hydrologic modeling and assessment part I: Model development. JAWRA J. Am. Water Resour. Assoc. 34 (1), 73–89. https://doi.org/10.1111/j.1752-1688.1998.tb05961.x.

Ashouri, H., Hsu, K.-L., Sorooshian, S., Braithwaite, D.K., Knapp, K.R., Cecil, L.D., Nelson, B.R., Prat, O.P., 2015. PERSIANN-CDR: daily precipitation climate data record frommultisatellite observations for hydrological and climate studies. Bull. Am. Meteorol. Soc. 96 (1), 69–83. https://doi.org/10.1175/BAMS-D-13-00068.1.

Awange, J., Ferreira, V., Forootan, E., Khandu, Andam-Akorful, S., Agutu, N., He, F., 2016. Uncertainties in remotely sensed precipitation data over Africa. Int. J. Climatol. 36, 303–323. https://doi.org/10.1002/joc.4346.

Ayehu, G.T., Tadesse, T., Gessesse, B., Dinku, T., 2018. Validation of new satellite rainfall products over the Upper Blue Nile Basin, Ethiopia. Atmos. Meas. Tech. 11, 1921–1936. https://doi.org/10.5194/amt-11-1921-2018.

Beck, H.E., van Dijk, A.I., De Roo, A., Miralles, D.G., McVicar, T.R., Schellekens, J., Bruijnzeel, L.A., 2016. Global-scale regionalization of hydrologic model parameters. Water Resour. Res. 52 (5), 3599–3622. https://doi.org/10.1002/2015WR018247.

Beck, H.E., Vergopolan, N., Pan, M., Levizzani, V., van Dijk, A.I.J.M., Weedon, G.P., Brocca, L., Pappenberger, F., Huffman, G.J., Wood, E.F., 2017. Global-scale evaluation of 22 precipitation datasets using gauge observations and hydrological modeling. Hydrol. Earth Syst. Sci. 21, 6201–6217. https://doi.org/10.5194/hess-21-6201-2017.

Beighley, R.E., Ray, R.L., He, Y., Lee, H., Schaller, L., Durand, M., Andreadis, K.M., Alsdorf, D.E., Shum, C.K., 2011. Comparing satellite derived precipitation datasets using the Hillslope River Routing (HRR) model in the Congo River Basin. Hydrol. Process. v. 25, 3216–3229. https://doi.org/10.1002/hyp.8045.

Bultot, F., 1971. Atlas Climatique du Bassin Congolais: Deuxième partie, les composantes du bilan d'eau. Publications de L'Institut National pour L'Etude Agronomique du Congo (I.N.E.A.C.).

Casse, C., Gosset, M., Peugeot, C., Pedinotti, V., Boone, A., Tanimoun, B.A., Decharme, B., 2015. Potential of satellite rainfall products to predict Niger River flood events in Niamey. Atmos. Res. 163, 162–176. https://doi.org/10.1016/j.atmosres.2015.01.010.

Crowhurst, D., Dadson, S., Peng, J., Washington, R., 2021. Contrasting controls on Congo Basin evaporation at the two rainfall peaks. Clim. Dyn. 56, 1609–1624. https://doi.org/10.1007/s00382-020-05547-1.

Datok, P., Fabre, C., Sauvage, S., N'kaya, G.M., Paris, A., Dos Santos, V., Laraque, A., Sánchez Pérez, J.-M., 2022. Investigating the role of the Cuvette Centrale in the hydrology of the Congo River Basin. In: Alsdorf, D., Moukandi, G., Tshimanga, R. (Eds.), Congo Basin Hydrology, Climate, and Biogeochemistry: A Foundation for the Future. Geophysical Monograph Series. John Wiley & Sons Inc, Hoboken, NJ, USA.

BRLi, 2016. Développement et mise en place de l'outil de modélisation et d'allocation des ressources en eau du Bassin du Congo: Rapport technique de construction et de calage du modèle. CICOS,, Kinshasa, RDC. https://www.cicos.int.

Dembélé, M., Schaefli, B., van de Giesen, N., Mariéthoz, G., 2020. Suitability of 17 gridded rainfall and temperature datasets for large-scale hydrological modelling in West Africa. Hydrol. Earth Syst. Sci. 24, 5379–5406. https://doi.org/10.5194/hess-24-5379-2020.

Dezfuli, A., Ichoku, C., Huffman, G., Mohr, K., Selker, J., Van DeGiesen, N, Hochreutener, R., Annor, F., 2017. Validation of IMERG Precipitation in Africa. Journal of Hydrometeorology 18 (10), 2817–2825. https://www.jstor.org/stable/26392114.

Dile, Y.T., Srinivasan, R., 2014. Evaluation of CFSR climate data for hydrologic prediction in data- scarce watersheds: an application in the Blue Nile River Basin. J. Am. Water Resour. Assoc. 50 (5), 1226–1241. https://doi.org/10.1111/jawr.12182.

Dos Santos, V., Laurent, F., Abe, C., Messner, F., 2018. Hydrologic response to land use change in a large basin in Eastern Amazon. Water 10, 1–19. https://doi.org/10.3390/w10040429.

Funk, C., Peterson, P., Landsfeld, M., Pedreros, D., Verdin, J., Shukla, S., Husak, G., Rowland, J., Harrison, L., Hoell, A., Michaelsen, J., 2015. The climate hazards infrared precipitation with stations - a new environmental record for monitoring extremes. Sci. Data 2, 1–21. https://doi.org/10.1038/sdata.2015.66.

Gosset, M., Alcoba, M., Roca, R., Urbani, G., Cloché, S., 2018. Evaluation of TAPEER daily estimates and other GPM era products against dense gauge networks in West Africa, analyzing ground reference uncertainty. Q. J. R. Meteorol. Soc. 144, 255–269. https://doi.org/10.1002/qj.3335.

Guilhen, J., Al Bitar, A., Sauvage, S., Parrens, M., Martinez, J.-M., Abril, G., Moreira-Turcq, P., Sanchez-Pérez, J.-M., 2020. Denitrification, carbon and nitrogen emissions over the Amazonian wetlands. Biogeosciences. https://doi.org/10.5194/bg-2020-3.

Gupta, H.V., Kling, H., Yilmaz, K.K., Martinez, G.F., 2009. Decomposition of the mean squared error and NSE performance criteria: implications for improving hydrological modelling. J. Hydrol. 377 (1–2), 80–91. https://doi.org/10.1016/j.jhydrol.2009.08.003.

Harris, N.L., Goldman, E., Gabris, C., Nordling, J., Minnemeyer, S., Ansari, S., Lippmann, M., Bennett, L., Raad, M., Hansen, M., Potapov, P., 2017. Using spatial statistics to identify emerging hot spots of forest loss. Environ. Res. Lett. 12, L024012 https://doi.org/10.1088/1748-9326/aa5a2f.

Hou, A.Y., Kakar, R.K., Neeck, S., Azarbarzin, A.A., Kummerow, C.D., Kojima, M., Oki, R., Nakamura, K., Iguchi, T., 2014. The global precipitation measurement mission. Bull. Am. Meteorol. Soc. 95 (5), 701–722. https://doi.org/10.1175/BAMS-D-13-00164.1.

Hua, W., Zhou, L., Nicholson, S.E., Chen, H., Qin, M., 2019. Assessing reanalysis data for understanding rainfall climatology and variability over Central Equatorial Africa. Clim. Dyn. 53, 651–669. https://doi.org/10.1007/s00382-018-04604-0.

Huffman, G.J., Adler, R.F., Morrissey, M.M., Bolvin, D.T., Curtis, S., Joyce, R., McGavock, B., Susskind, J., 2001. Global precipitation at one-degree daily resolution frommultisatellite observations. J. Hydrometeorol. 2 (1), 36–50. https://doi.org/10.1175/1525-7541(2001)002<0036:GPAODD>2.0.CO;2.

Huffman, G.J., Bolvin, D.T., Nelkin, E.J., Wolff, D.B., Adler, R.F., Gu, G., Hong, Y., Bowman, K.P., Stocker, E.F., 2007. The TRMM multisatellite precipitation analysis (TMPA):quasi-global, multiyear, combined-sensor precipitation estimates atfine scales. J. Hydrometeorol. 8 (1), 38–55. https://doi.org/10.1175/JHM560.1.

Huffman, G.J., Bolvin, D.T., Braithwaite, D., Hsu, K.L., Joyce, R., Kidd, C., Nelkin, E.J., Sorooshian, S., Tan, J., Xie, P., 2019. Algorithm Theoretical Basis Document (ATBD) Version 06 NASA Global Precipitation Measurement (GPM) Integrated Multi-satellitE Retrievals for GPM (IMERG). National Aeronautics and Space Administration (NASA), Washington, DC, USA, pp. 1–34.

Jackson, B., Nicholson, S.E., Klotter, D., 2009. Mesoscale convective systems over western equatorial Africa and their relationship to large-scale circulation. Mon. Weather Rev. 137, 1272–1294. https://doi.org/10.1175/2008MWR2525.1.

Kabuya, P.M., Hughes, D.A., Tshimanga, R.M., Trigg, M.A., Bates, P., 2020. Establishing uncertainty ranges of hydrologic indices across climate and physiographic regions of the Congo River Basin. Journal of Hydrology: Regional Studies 30, 100710. https://doi.org/10.1016/j.ejrh.2020.100710.

KGE-hydroGOF. 2017. "Kling–Gupta Efficiency." https://www.rforge.net/doc/packages/hydroGOF/KGE.html.

Kidd, C., Levizzani, V., 2011. Status of satellite precipitation retrievals. Hydrol. Earth Syst. Sci. 15, 1109–1116. https://doi.org/10.5194/hess-15-1109-2011.

Kidd, C., Becker, A., Huffman, G.J., Muller, C.L., Joe, P., Skofronick-Jackson, G., Kirschbaum, D.B., 2017. So, how much of the earth's surface is covered by rain gauges? Bull. Am. Meteorol. Soc. 98 (1), 69–78. https://doi.org/10.1175/BAMS-D-14-00283.1.

Knoben, W.J.M., Freer, J.E., Woods, R.A., 2019. Technical note: Inherent benchmark or not? Comparing Nash-Sutcliffe and Kling-Gupta efficiency scores. Hydrol. Earth Syst. Sci. 23 (10), 4323–4331. https://doi.org/10.5194/hess-23-4323-2019.

Kubota, T., Shige, S., Hashizume, H., Aonashi, K., Takahashi, N., Seto, S., Hirose, M., Takayabu, Y.N., Ushio, T., Nakagawa, K., Iwanami, K., Kachi, M., Okamoto, K., 2007. Global precipitation map using satellite-borne microwave radiometers by the GSMaP project: production and validation. IEEE 5 Trans. Geosci. Remote Sens. 45 (7), 2259–2275. https://doi.org/10.1109/tgrs.2007.895337.

Laraque, A., Mahé, G., Orange, D., Marieu, B., 2001. Spatiotemporal variations in hydrological regimes within Central Africa during the XXth century. J. Hydrol. 245 (1–4), 104–117. https://doi.org/10.1016/S0022-1694(01)00340-7.

Liu, Y., Yang, W., Wang, X., 2008. Development of a SWAT extension module to simulate riparian wetland hydrologic processes at a watershed scale. Hydrol. Process. 22 (16), 2901–2915. https://doi.org/10.1002/hyp.6874.

Loucks, D.P., Van Beek, E., 2017. An Introduction to Probability, Statistics, and Uncertainty. In: Water Resource Systems Planning and Management, 2017. Springer, Cham, pp. 51–72. https://doi.org/10.1007/978-3-319-44234-1.

Maggioni, V., Massari, C., 2018. On the performance of satellite precipitation products in riverine flood modeling: a review. J. Hydrol. 558, 214–224. https://doi.org/10.1016/j.jhydrol.2018.01.039.
Maidment, R.I., Grimes, D., Black, E., Tarnavsky, E., Young, M., Greatrex, H., Allan, R.P., Stein, T., Nkonde, E., Senkunda, S., Alcántara, E.M.U., 2017. A new, long-term daily satellite-based rainfall dataset for operational monitoring in Africa. Sci. Data 4, 1–19. https://doi.org/10.1038/sdata.2017.63.
McCollum, J.R., Gruber, A., Ba, M.B., 2000. Discrepancy between gauges and satellite estimates of rainfall in equatorial Africa. J. Appl. Meteor. 39, 666–679. https://doi.org/10.1175/1520-0450-39.5.666.
Melaku, N.D., Wang, J., 2019. A modified SWAT module for estimating groundwater table at Lethbridge and Barons, Alberta, Canada,. Journal of Hydrology 575, 420–431. https://doi.org/10.1016/j.jhydrol.2019.05.052.
Moradkhani, H., Sorooshian, S., 2008. General review of rainfall-runoff modeling: Model calibration, data assimilation, and uncertainty analysis. In: Sorooshian, S., Hsu, K.L., Coppola, E., Tomassetti, B., Verdecchia, M., Visconti, G. (Eds.), Hydrological Modelling and the Water Cycle, 63. Springer, Berlin/Heidelberg, Germany, pp. 1–24.
Moriasi, D.N., Gitau, M.W., Pai, N., Daggupati, P., 2015. Hydrologic and water quality models: performance measures and evaluation criteria. Trans. ASABE 58, 1763–1785. https://doi.org/10.13031/trans.58.10715.
Moriasi, D.N., Arnold, J.G., van Liew, M.W., Bingner, R.L., Harmel, R.D., Veith, T.L., 2007. Model evaluation guidelines for systematic quantification of accuracy in watershed simulations. Trans. ASABE 50, 885–900. https://doi.org/10.13031/2013.23153.
Moukandi N'kaya, G.D., Laraque, A., Paturel, J.M., Gulemvuga, G., Mahé, G., Tshimanga Muamba, R., 2021. A new look at hydrology in the Congo Basin, based on the study of multi- decadal chronicles. In: Alsdorf, D., Tshimanga Muamba, R., Moukandi N'kaya, G.D. (Eds.), Congo Basin Hydrology, Climate, and Biogeochemistry: A Foundation for the Future, AGU Geophysical Monograph Series. John Wiley & Sons Inc, Hoboken, NJ.
Munzimi, Y.A., Hansen, M.C., Adusei, B., Senay, G.B., 2015. Characterizing Congo basin rainfall and climate using Tropical Rainfall Measuring Mission (TRMM) satellite data and limited rain gauge ground observations. J. Appl. Meteorol. Climatol. 54, 541–555. https://doi.org/10.1175/JAMC-D-14-0052.1.
Nash, J.E., Sutcliffe, J.V., 1970. River flow forecasting through conceptual model. Part 1-A Discussion of principles. J. Hydrol. 10, 282–290. https://doi.org/10.1016/0022-1694(70)90255-6.
Negron Juarez, R.I.N., Li, W.H., Fu, R., Fernandes, K., Cardoso, A.D., 2009. Comparison of precipitation datasets over the tropical South American and African continents. J. Hydrometeor. 10, 289–299. https://doi.org/10.1175/2008JHM1023.1.
Neitsch, S, Arnold, J, Kiniry, J, Williams, J, 2011. Soil & Water Assessment Tool Theoretical Documentation Version 2009. Texas Water Resources Institute 1–647. https://doi.org/10.1016/j.scitotenv.2015.11.063.
Nicholson, S.E., Klotter, D., Zhou, L., Hua, W., 2019. Validation of satellite precipitation estimates over the Congo Basin. J. Hydrometeorol. 20 (4), 631–656. https://doi.org/10.1175/JHM-D-18-0118.1.
Novella, N.S., Thiaw, W.M., 2013. African rainfall climatology version 2 for famine early warning systems. J. Appl. Meteorol. Climatol. 52, 588–606. https://doi.org/10.1175/JAMC-D-11-0238.1.
Oliveira, R., Maggioni, V., Vila, D., Morales, C., 2016. Characteristics and diurnal cycle of GPM rainfall estimates over the Central Amazon Region. Remote Sens. 8, 544. https://doi.org/10.3390/rs8070544.
Pagliero, L., Bouraoui, F., Willems, P., Diels, J., 2014. Large-scale hydrological simulations using the soil water assessment tool, protocol development, and application in the danube basin. Journal of Environmental Quality 43 (1), 145–154. https://doi.org/10.2134/jeq2011.0359.
Peng, J., Liu, T., Huang, Y., Ling, Y., Li, Z., Bao, A., Chen, X., Kurban, A., De Maeyer, P., 2021. Satellite-based precipitation datasets evaluation using gauge observation and hydrological modeling in a typical arid land watershed of Central Asia. Remote Sens. 13, 221. https://doi.org/10.3390/rs13020221.
Phiri, W.K., Vanzo, D., Banda, K., Nyirenda, E., Nyambe, I.A., 2021. A pseudo-reservoir concept in SWAT model for the simulation of an alluvial floodplain in a complex tropical river system. J. Hydrol. Reg. Stud. 33, 100770 https://doi.org/10.1016/j.ejrh.2020.100770.
Roca, R., 2019. Estimation of Extreme Daily Precipitation Thermodynamic Scaling Using Gridded Satellite Precipitation Products Over Tropical Land. Environ. Res. Lett. IOP Publishing, p. 14. https://doi.org/10.1088/1748-9326/ab35c6.
Roca, R., Chambon, P., Jobard, I., Kirstetter, P., Gosset, M., Bergès, J.C., 2010. Comparing satellite and surface rainfall products over West Africa at meteorologically relevant scales during the AMMA campaign using error estimates. J. Appl. Meteorol. Climatol. 49 (4), 715–731. https://doi.org/10.1175/2009JAMC2318.1.
Roca, R., Alexander, L.V., Potter, G., Bador, M., Jucá, R., Contractor, S., Bosilovich, M.G., Cloché, S., 2019. FROGS: a daily $1^\circ \times 1^\circ$ gridded precipitation database of rain gauge, satellite and reanalysis products, Earth Syst. Sci. Data 11, 1017–1035. https://doi.org/10.5194/essd-11-1017-2019.
Runge, J., 2007. The Congo River, Central Africa, in Large Rivers: Geomorphology and Management. In: Gupta, A. (Ed.), Large Rivers. Wiley, U.K, pp. 293–309. https://doi.org/10.1002/9780470723722.ch14.
Satgé, F.D., Defrance, B.S., Bonnet, M.P., Seyler, F., Rouché, N., Pierron, F., Paturel, J.E., 2020. Evaluation of 23 gridded precipitation datasets across West Africa. J. Hydrol. 581, 124412 https://doi.org/10.1016/j.jhydrol.2019.124412.
Shao, G., Guan, Y., Zhang, D., Yu, B., Zhu, J., 2018. The impacts of climate variability and land use change on streamflow in the Hailiutu River Basin. Water 10, 814. https://doi.org/10.3390/w10060814.
Sharannya, T.M., Al-Ansari, N., Deb Barma, S., Mahesha, A., 2020. Evaluation of satellite precipitation products in simulating streamflow in a humid tropical catchment of India using a semi-distributed hydrological model. Water 12, 2400. https://doi.org/10.3390/w12092400.
USDA Soil Conservation Service, 1972. National Engineering Handbook; Section 4, Hydrology, Chapter 21. USDA Soil Conservation Service, Washington, DC, USA.
Skofronick-Jackson, G., Petersen, W.A., Berg, W., Kidd, C., Stocker, E.F., Kirschbaum, D.B., Kakar, R., Braun, S.A., Huffman, G.J., Iguchi, T., Kirstetter, P.E., Kummerow, C., Meneghini, R., Oki, R., Olson, W.S., Takayabu, Y.N., Kurukawa, K., Wilheit, T., 2017. The Global Precipitation Measurement (GPM) mission for science and society. Bull. Am. Meteorol. Soc. 98, 1679–1695. https://doi.org/10.1175/BAMS-D-15-00306.1.
Strauch, M., Volk, M., 2013. SWAT plant growth modification for improved modeling of perennial vegetation in the tropics. Ecol. Model. 269, 98–112. https://doi.org/10.1016/j.ecolmodel.2013.08.013.
Sun, Q., Miao, C., Duan, Q., Ashouri, H., Sorooshian, S., Hsu, K.L., 2017. A review of global precipitation datasets: data sources, estimation, and intercomparisons, 79–10 Rev. Geophys. 56. https://doi.org/10.1002/2017RG000574.
Sun, X., Bernard-Jannin, L., Garneau, C., Volk, M., Arnold, J.G., Srinivasan, R., Sauvage, S., Sanchez-Perez, J.-M., 2015. Improved simulation of river water and groundwater exchange in an alluvial plain using the SWAT model. Hydrol. Process. 30 (2), 187–202. https://doi.org/10.1002/hyp.10575.
Tan, M.L., Yang, X., 2020. Effect of rainfall station density, distribution and missing values on SWAT outputs in tropical region. J. Hydrol. 584, 124660 https://doi.org/10.1016/j.jhydrol.2020.124660.
Tan, M.L., Samat, N., Chan, N.W., Roy, R., 2018. Hydro-meteorological assessment of three GPM satellite precipitation products in the Kelantan River Basin, Malaysia. Remote Sens. 10, 1011. https://doi.org/10.3390/rs10071011.
Tshimanga, R.M., Hughes, D.A., 2014. Basin-scale performance of a semi-distributed rainfall-runoff model for hydrological predictions and water resources assessment of large rivers: the Congo River. Water Resour. Res. 50, 1174–1188. https://doi.org/10.1002/2013WR014310.
Tshimanga, R.M., Hughes, D.A., Kapangaziwiri, E., 2012. Initial calibration of a semi-distributed rainfall runoff model for the Congo River basin. Phys. Chem. Earth 36, 761–774. https://doi.org/10.1016/j.pce.2012.08.002.
Tuo, Y., Duan, Z., Disse, M., Chiogna, G., 2016. Evaluation of precipitation input for SWATmodeling in Alpine catchment: a case study in the Adige river basin (Italy). Sci. Total. 573, 66–82. https://doi.org/10.1016/j.scitotenv.2016.08.034.
Wagner, P.D., Kumar, S., Fiener, P., Schneider, K., 2011. Technical Note: Hydrological Modeling with SWAT in a Monsoon-Driven Environment: Experience from theWestern Ghats, India. Trans. ASABE 54, 1783–1790. https://doi.org/10.13031/2013.39846.
Wang, Q., Xia, J., She, D., Zhang, X., Liu, J., Zhang, Y., 2021. Assessment of four latest long-term satellite-based precipitation products in capturing the extreme precipitation and streamflow across a humid region of southern China. Atmos. Res. 257, 105554 https://doi.org/10.1016/j.atmosres.2021.105554.
Williams, J.R., 1969. Flood routing with variable travel time or variable storage coefficients. Trans. ASABE 12, 100–0103. https://doi.org/10.13031/2013.38772.
Winchell, M., Srinivasan, R., Di Luzio, M., Arnold, J.G., 2013. Arcswat Interface for SWAT2012: User's Guide; Blackland Research Center. Texas AgriLife Research: Temple, TX, USA.

Xie, P., Joyce, R., Wu, S., Yoo, S.H., Yarosh, Y., Sun, F., Lin, R., 2017. Reprocessed, bias-corrected CMORPH global high-resolution precipitation estimates from 1998. J. Hydrometeorol. 18, 1617–1641. https://doi.org/10.1175/JHM-D-16-0168.1.

Yin, X., Gruber, A., 2010. Validation of the abrupt change in GPCP precipitation in the Congo River Basin. Int. J. Climatol. 30 (1), 110–119. https://doi.org/10.1002/joc.1875.

Yin, X., Gruber, A., Arkin, P., 2004. Comparison of the GPCP and CMAP merged gauge–satellite monthly precipitation products for the period 1979–2001. J. Hydrometeorol. 5 (6), 1207–1222. https://doi.org/10.1175/JHM-392.1.

Zhou, L., Tian, Y., Myneni, R., Ciais, P., Saatchi, S., Liu, Y.Y., Piao, S., Chen, H., Vermote, E.F., Song, C., Hwang, T., 2014. Widespread decline of Congo rainforest greenness in the past decade. Nature 509, 86–90. https://doi.org/10.1038/nature13265.